



FORM EG&G 398
(Rev. 11-79)

INTERIM REPORT

Accession No. _____

Report No. EGG-TFBP-5251

Contract Program or Project Title: Thermal Fuels Behavior Program

Subject of this Document: MEASURED RELEASE OF RADIOACTIVE XENON, KRYPTON AND IODINE
FROM UO₂ DURING NUCLEAR OPERATION AND A COMPARISON WITH
RELEASE MODELS

Type of Document: Preliminary

Author(s): A. D. Appelhans
J. A. Turnbull

Date of Document: September 1980

Responsible NRC Individual and NRC Office or Division: G. P. Marino

This document was prepared primarily for preliminary or internal use. It has not received full review and approval. Since there may be substantive changes, this document should not be considered final.

EG&G Idaho, Inc.
Idaho Falls, Idaho 83415

Prepared for the
U.S. Nuclear Regulatory Commission
Washington, D.C.
Under DOE Contract No. DE-AC07-76ID01570
NRC FIN No. A6041

INTERIM REPORT

8010300178

NRC Research and Technical
Assistance Report

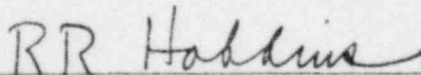
MEASURED RELEASE OF RADIOACTIVE
XENON, KRYPTON AND IODINE FROM
UO₂ DURING NUCLEAR OPERATION
AND A COMPARISON WITH
RELEASE MODELS

By

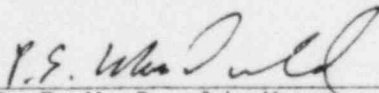
A. D. Appelhans J. A. Turnbull^a

September 1980

Approved:



R. R. Hobbins, Manager
Program Development and Evaluation Branch



P. E. MacDonald, Manager
Light Water Reactor Fuel Research Division

a. On assignment at the Halden Reactor Project from the CEGB Berkeley Nuclear Laboratories, U.K.

SUMMARY

The amount of radioactive fission products in the fuel-cladding gap of light water reactor (LWR) fuel rods, the gap inventory, which is available for release should the cladding fail, is one of the Nuclear Regulatory Commission's (NRC's) current licensing issues. The current Regulatory Guide 1.25, 1.3, and 1.4 assumptions of 100% release of noble gases and 25% release of iodine for loss of coolant type accidents and 10% release of noble gases and iodine during fuel handling accidents, have been estimated by the NRC to be over-conservative by factors of 100 and 10, respectively.

Direct measurement of the gap inventory during irradiation provides the data necessary to assess the conservatism of the Regulatory Guides and check the predictions of models being developed to calculate the gap inventory. As part of the NRC's Water Reactor Safety Research Fuel Behavior Program, EG&G Idaho, Inc. is conducting fuel behavior experiments in the Halden Reactor in Halden, Norway. The Instrumented Fuel Assembly-430 (IFA-430) operated in that facility is designed to provide data on the release of xenon, krypton and iodine fission products to the fuel-cladding gap during irradiation.

This report presents the results of the initial measurements of short-lived Xe, Kr and I release fractions, compares the measured data with release fractions predicted by the proposed American Nuclear Society Standard ANS 5.4 model for fission gas release and by the diffusion model of Turnbull and Friskney, and compares the measured and calculated release fractions with the NRC Regulatory Guide assumptions.

The IFA-430 test assembly contains four 1.28 m long fuel rods loaded with 10% enriched UO_2 pellet fuel. Two of the rods are used in fission gas release experiments, each is instrumented with a centerline thermocouple and three axially spaced pressure sensors. These two rods are of typical LWR design with diametral gap sizes of 0.23 mm and 0.10 mm representing beginning of life and end of life conditions, respectively. The rods are connected to a gas flow system which permits the fission gases

released to the gap to be swept out of the fuel rods to a gamma spectrometer where the isotopic content is quantitatively measured.

The steady state equilibrium release rate of Xe and Kr isotopes were measured at an average fuel rod heating rate of ~ 23 kW/m, with fuel centerline temperatures of ~ 1350 K, at a burnup of 4500 MWd/t. The release fractions of ^{131}I , ^{133}I , and ^{135}I were measured for similar conditions at burnup of 5000 MWd/t. The measured release fractions for Xe ranged from 1.6×10^{-5} for ^{137}Xe to 3.3×10^{-4} for ^{133}Xe and for Kr ranged from 1.5×10^{-5} for ^{89}Kr to 8.0×10^{-5} for $^{85\text{m}}\text{Kr}$. The measured release fractions for iodine were 4.2×10^{-5} for ^{135}I , 1.5×10^{-3} for ^{133}I and 2.3×10^{-4} for ^{131}I ; the measured release fraction for ^{133}I is unexpectedly high, by a factor of about 10, and is questionable at this time.

The ANS 5.4 predicted release fractions for ^{135}Xe and ^{133}Xe are within the uncertainty band of the data; however, for shorter lived (<15 min) isotopes the predicted release is low by a factor of about 2. For krypton the ANS 5.4 predicted release fraction is low by a factor of 2 to 4. The iodine release fraction calculated with ANS 5.4 is within a factor of 2 of the measured values for ^{135}I and ^{131}I .

The diffusion model of Turnbull and Friskney, which takes precursor effects into account, predicts noble gas release fractions which show very good agreement with the data when the fuel pellets are assumed to contain about seven radial cracks. More significantly, the model predicts the detailed relationship between the different isotopes due to precursor effects and element dependent diffusion coefficients, indicating the model probably includes the correct mechanisms.

A comparison of the order of magnitude of the measured and calculated release fractions, generally 10^{-4} to 10^{-3} , with the NRC Regulatory Guide assumptions of 0.1 for fuel handling type accidents confirms the NRC estimate that the Regulatory Guide assumption is overly-conservative. For successfully terminated LOC type accidents for which fuel temperatures remain below ~ 1400 K the data and calculations also support the NRC estimate that the Regulatory Guide assumed release fraction of 1.0 is high by a factor of 100.

ACKNOWLEDGEMENT

The experiments reported herein were funded by the United States Nuclear Regulatory Commission; the support of that organization and particularly Dr. G. P. Marino is appreciated. Many people have provided their assistance: R. J. Gehrke in spectrometer calibration; W. Olsen in setting up and running the ORIGEN code; G. Berna in modifying and running the FRAPCON code; R. Miller, E. Skattum, T. Johnson, and J. Aasgard in data collection and experiment operation; and G. Reilly in data processing. Their assistance is gratefully acknowledged.

CONTENTS

| | |
|---|-----|
| SUMMARY | iii |
| ACKNOWLEDGEMENT | v |
| 1. INTRODUCTION. | 1 |
| 2. EXPERIMENT DESIGN AND CONDUCT | 4 |
| 2.1 IFA-430 Irradiation Assembly and FPMS. | 4 |
| 2.2 Experiment Conduct | 9 |
| 3. EXPERIMENT RESULTS. | 13 |
| 3.1 Noble Gases. | 13 |
| 3.2 Iodine Release | 18 |
| 4. DISCUSSION OF RELEASE MECHANISMS. | 20 |
| 5. COMPARISON WITH RELEASE MODELS. | 23 |
| 5.1 ANS 5.4 | 23 |
| 5.2 Diffusion Model. | 27 |
| 6. DISCUSSION AND CONCLUSIONS. | 36 |
| 7. REFERENCES. | 39 |
| APPENDIX A - Release Rate Calculations. | 41 |
| APPENDIX B - Summary of ORIGEN Calculations | 49 |
| APPENDIX C - Typical Gamma-Ray Spectrum Analysis. | 58 |
| APPENDIX D - Uncertainty Analysis | 61 |

INTRODUCTION

One of the Nuclear Regulatory Commission's (NRC) current^{1,2} licensing issues is the amount of radioactive fission products in the fuel-cladding gap of light water reactor (LWR) fuel rods which is available for release should the fuel rod fail. Successfully terminated loss-of-coolant and operational transient type accidents, as well as fuel handling and transportation accidents, may result in release of the volatile fission products present in the fuel-cladding gap; however, only a small percent of the volatile fission products produced in the fuel are realistically expected to be in the gap and, therefore available for release.

Currently the releases assumed for a loss-of-coolant type accident (Regulatory Guides 1.3 and 1.4) are estimated¹ to be about 100 times too large; and releases assumed for most other accidents (Regulatory Guide 1.25) are estimated¹ to be about 10 times too large. Thus direct measurement of fuel-cladding gap fission product inventory is necessary for evaluating the fuel licensing issues and assessing the potential consequences of fuel cladding failure both during postulated reactor transients and during handling and transportation of spent fuel.

The American Nuclear Society (ANS) proposed standard ANSI/ANS-5.4³ for calculating the release of fission products is being used in the GAPCON-2⁴ fuel behavior code to provide a basis for revising the NRC regulatory guides. However, the ANS has found that "insufficient data exist to directly determine a release correlation for short-lived isotopes," and have used stable-gas-release data to develop a model which is extended to include radioactive species. The extension of the stable-gas-release models to short lived radioactive gases and volatiles should be checked by comparing the predicted release fractions with measured release fractions.

A part of the NRC Reactor Safety Research Program⁵ includes studies of UO_2 fission product release in the Heavy Boiling Water Reactor

(HBWR) in Halden, Norway. The HBWR was built by the Norwegian Institute for Atomenergi, and has been operated by the Organization for Economic Cooperation and Development Halden Reactor Project through an international agreement between participating governments and organizations. One of the assemblies being irradiated in the HBWR is the Instrumented Fuel Assembly-430 (IFA-430) managed by EG&G Idaho, Inc. for the NRC. IFA-430 was designed to provide fuel rod axial gas flow, fuel temperature, and fission gas release data for LWR fuel rods.

The purpose of this report is to present the results of a preliminary analysis of fission gas release to the fuel-cladding gap using measured fission gas release data from IFA-430. In particular, the report is intended to document the test procedures and results, compare the measured fission gas release fractions with the predictions of current models, and briefly discuss the significance of the results to reactor safety and licensing criteria.

The IFA-430 consists of four LWR-type fuel rods. Two rods (Rods 2 and 4), termed gas flow rods, each have three axially distributed pressure transducers mounted directly to the cladding, a centerline thermocouple, and each is connected to an external gas supply system that allows gas to be forced through the rod. The gas flow system provides a means for the fission gases released to the fuel-cladding gap to be swept out of the rod and to a fission product monitoring system where the isotopic content of the gas stream is quantitatively measured using a gamma spectrometer.

The IFA-430 is unique in that it provides fission gas release data for a representative LWR type fuel rod during actual nuclear operation. Other fission gas release experiments have included measurements on small specimens of UO_2 (single crystals,⁶ small cylinders,⁷ small spheres,^{8,9} and single pellets¹⁰), and the results have been used to develop various models for fission gas release. The IFA-430 data are used to assess the applicability of the models to a typical LWR type fuel rod.

The data for this analysis were obtained at a burnup of ~ 4500 MWd/t at average power levels of 22 to 23.5 kW/m. The peak fuel centerline

temperatures were ~ 1350 K; the bulk average fuel temperature was ~ 350 K. The isotopic release rates for Xe and Kr were measured at steady state conditions at three different occasions during a one week period; the reactor had been at constant power for sufficient time to allow the Xe and Kr isotopes used in the analysis to come to equilibrium prior to the fission gas release tests. The steady state release rates were determined by flowing a constant stream of He ($16 \text{ cm}^3/\text{s}$) through each fuel rod and acquiring 4 to 5 measurements of the content of the gas stream using on-line gamma spectroscopy.

The release of volatile iodine was measured indirectly by measuring the Xe decay products of the iodine isotopes following reactor shutdown. The technique permits the steady state release rate of ^{135}I and the release fraction of ^{131}I , and ^{133}I , and to be determined.

The experiment design and conduct are described in Section 2 and the results of the experiments are presented in Section 3. Section 4 contains a discussion of the release mechanisms. A comparison of the measured release fractions with the predictions of the ANS 5.4 model and the diffusion model of Friskney and Turnbull are presented in Section 5. A brief discussion of the implications of the results to the NRC licensing criteria and conclusions are presented in Section 6. The appendices contain details of the release rate calculation methodology, typical gamma spectra, the birth rate calculations, and an uncertainty analysis.

2. EXPERIMENT DESIGN AND CONDUCT

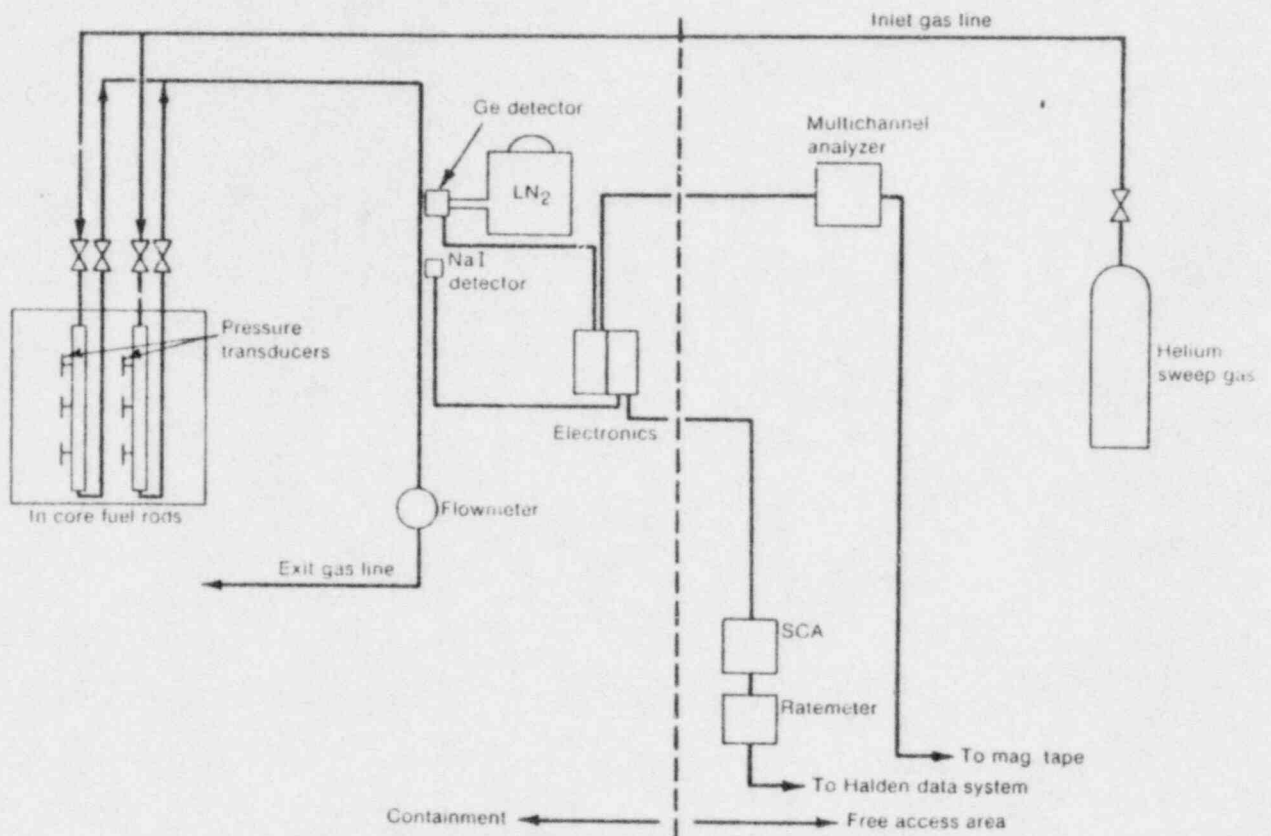
The fission gas release experiments are performed using the IFA-430 assembly and fission product measurement system (FPMS). A detailed description of the design and operation of the IFA-430 assembly is provided in Reference 11 and of the FPMS in Reference 12; a summary is provided in this section along with a description of the experiment conduct.

2.1 IFA-430 Irradiation Assembly and FPMS

IFA-430 contains four, 1.28-m-long fuel rods containing 10% enriched UO_2 fuel pellets. Two of the rods in the assembly are termed gas flow rods. The gas flow rods each have a fuel centerline thermocouple and three axially spaced pressure sensors and are connected to a gas flow system, shown in Figure 1, which is used during fission gas release experiments to sweep the fission gases out of the fuel rods and to the FPMS. A schematic of the gas flow rods is shown in Figure 2. The other two rods, not used in the fission gas release tests, are each equipped with two centerline thermocouples and three off-center thermocouples and are pressurized to 0.48 MPa with helium. Table 1 presents the IFA-430 fuel rod instrumentation and design parameters; Figure 3 shows the assembly instrumentation.

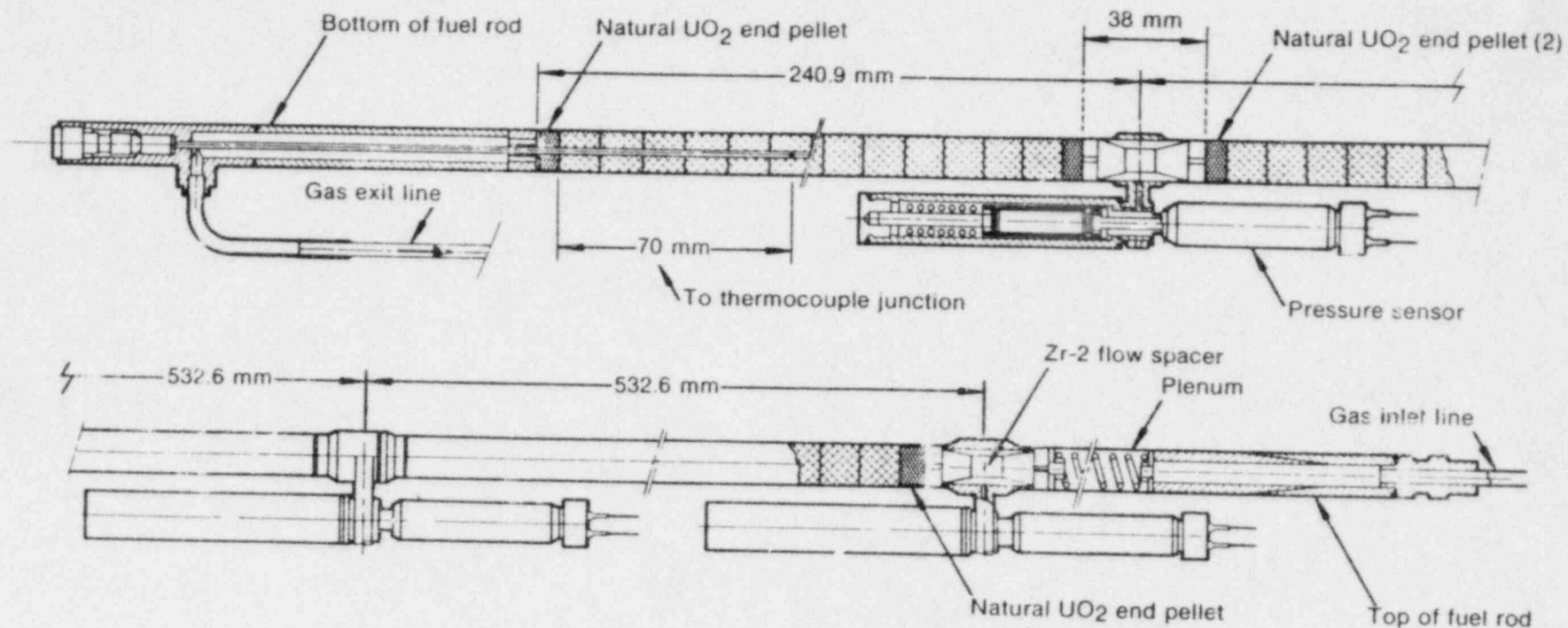
The gas flow system is capable of providing a wide range of steady state flow rates (8 to 800 cm^3/s). Helium is used as the sweep gas during the fission gas release tests. The gas flow is a once-through process: gas introduced from regulated high pressure cylinders sweeps the released fission gases from either one of the gas flow fuel rods to the FPMS detector station where the isotopic fission gas content is measured.

The fission product measurement system was designed to measure the quantitative release of fission gases from the fuel to the fuel-cladding gap. Fission gases swept from the fuel-cladding gap with a carrier gas are routed to the FPMS detector station where the fission gases contained in



INEL-A-10 093

Figure 1. IFA-430 gas flow system simplified piping diagram and FPMS instrumentation.



INEL-B-11 003

Figure 2 Location of fuel centerline thermocouple and rod pressure sensors on gas flow rods.

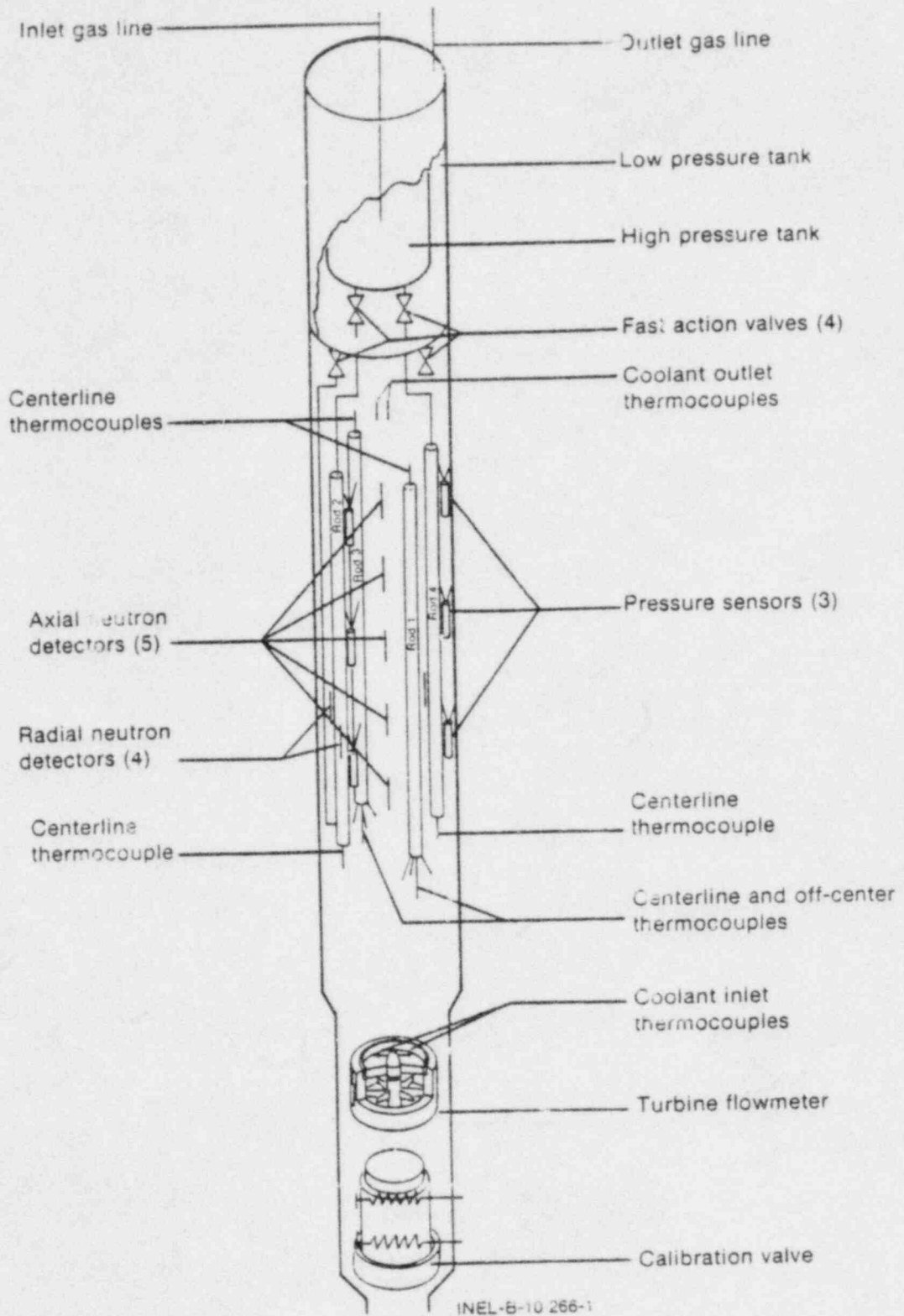


Figure 3 IFA-430 assembly in core instrumentation.

TABLE 1. IFA-430 FUEL ROD INSTRUMENTATION AND DESIGN VARIABLES

| Rod | Experiment | Diametral Gap | Fill Gas | Instrumentation |
|-----|------------------|---------------|-------------|--|
| 1 | Fuel temperature | 0.229 mm | 0.48 MPa He | 2 centerline thermocouples, 3 off-center thermocouples |
| 2 | Gas release | 0.229 mm | variable | centerline thermocouple, 3 pressure sensors |
| 3 | Fuel temperature | 0.102 mm | 0.48 MPa He | 2 centerline thermocouples, 3 off-center thermocouples |
| 4 | Gas release | 0.102 mm | variable | centerline thermocouples, 3 pressure sensors |

Fuel--Form - pressed and sintered UO₂ pellets
 Enrichment - 10 weight percent U-235
 Density - 10.412 g/cc (95% of theoretical)
 Shape - length, 12.7 mm
 - diameter, 10.808 mm, 10.681 mm
 - ends, chamfered 45° to an approximate depth of 0.12 mm

Cladding--zircaloy-2
 OD - 12.79 mm
 ID - 10.91 mm

the gas stream are measured as they flow by a gamma spectrometer. Gamma-ray spectra are stored on magnetic disk and tape and, after the experiments, are analyzed to determine the quantitative release rate of Kr and Xe isotopes and, under special conditions isotopes of I. To ensure that data collected during experiments are suitable for analysis and to track the behavior of the experiments as they progress, the data stored on disk are analyzed throughout the experiments using the data acquisition system microcomputer. The fuel centerline temperature and fuel rod power are recorded on one of the three Halden Reactor data acquisition systems.

2.2 Experiment Conduct

The Xe and Kr fission gas release measurements were conducted during a four day period in January 1980. Measurement of ^{135}I was made following the scram of January 6, and measurement of ^{131}I and ^{133}I were made on April 25, 1980, following a reactor shutdown.

The Xe and Kr gas release measurements were performed following a two week period of constant reactor power; this insured that all of the isotopes measured, except for ^{133}Xe , were at equilibrium and thus the release rates constant. The fuel had attained a burnup of ~ 4500 MWd/t at the time the experiments were conducted and the peak fuel temperatures had not exceeded 1560 K during this burnup. The fuel pellets were pressed and sintered UO_2 with a fabricated grain size ranging from ~ 0.02 mm at the outer radius to ~ 0.07 mm in the middle of the pellet.¹¹ The peak fuel centerline temperature during the fission gas release tests were ~ 1350 K; the bulk average fuel temperature was ~ 850 K. The average linear heat ratings of the fuel rods were 22 to 23.5 kW/m (~ 25 W/g) with a peak-to-average of 1.2. Figure 4 shows the rod power history for the operating period when the tests were conducted.

The steady state fission gas release rates were measured by flowing helium gas through each fuel rod at flow rates ranging from 8.3 to 50.0 cm^3/s and acquiring 4 to 5 gamma ray spectra at each flow rate. The measurements were performed on the 14th, 15th, and 17th day of constant power operation prior to the scram on January 6.

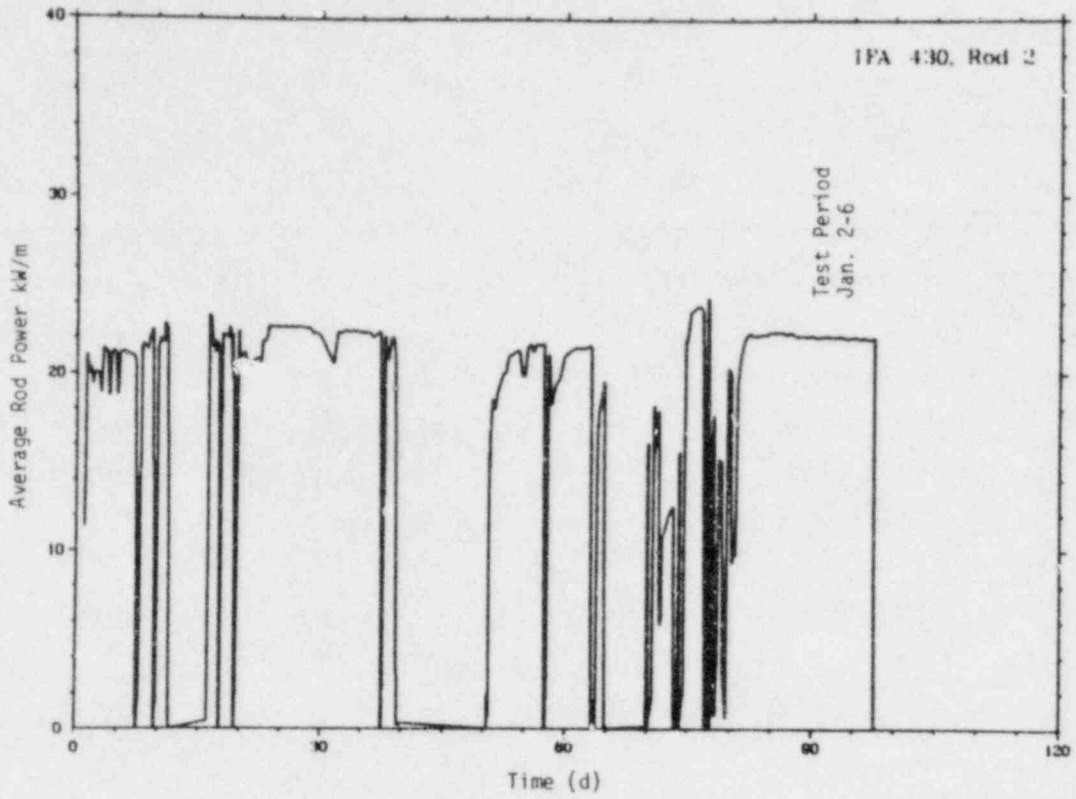


Figure 4. Rod 2 average power from Oct. 1, 1979 through Jan. 31, 1980.

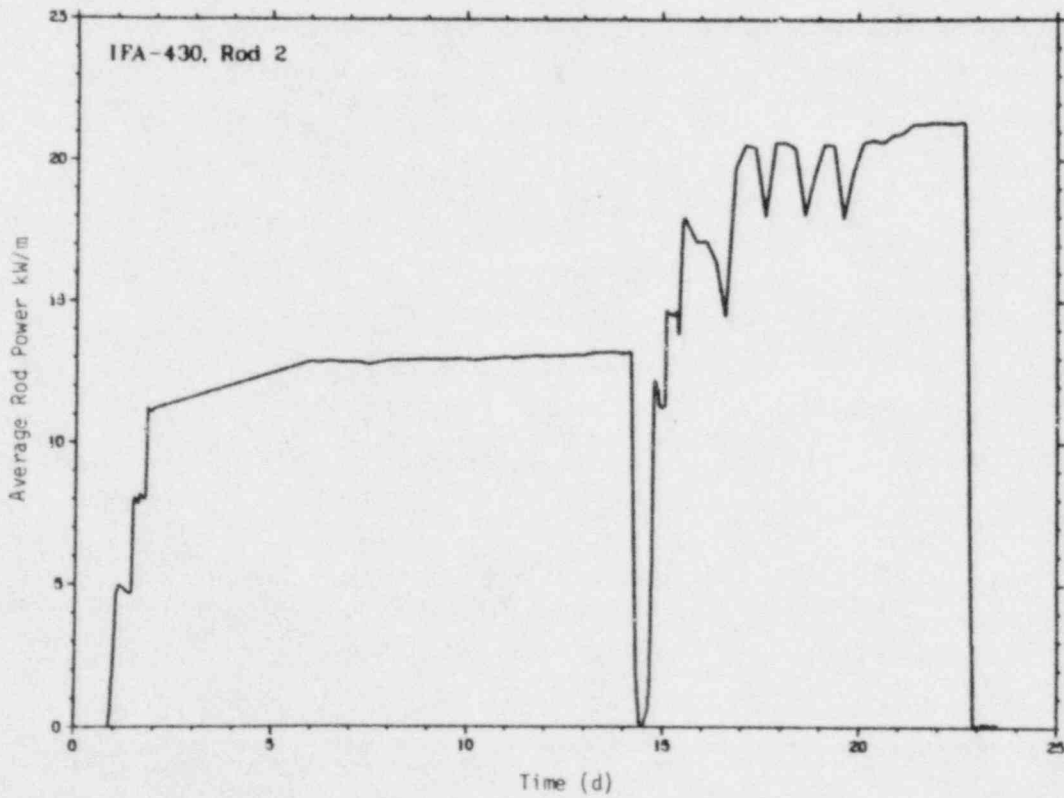


Figure 5. Rod 2 average power from March 28 through April 18, 1980.

The isotopic iodine release rate cannot be measured directly because iodine plates out on the fuel and cladding surface and is not transported in the gas stream to the FPMS. However, the iodine release rate and the gap inventory were determined by measuring the iodine decay products, i.e. the xenon isotopes. Two procedures were used to determine the gap inventory of the three significant iodine isotopes.

The technique described by Carroll¹⁷ was used to measure the ^{135}I release rate. The ^{135}Xe release measured at steady state power consists of ^{135}Xe released from the UO_2 in its gaseous state and ^{135}Xe coming from the decay of ^{135}I plated out on the fuel and cladding surfaces. A stable ^{135}Xe release rate indicates that both the release of ^{135}Xe from the fuel as a gas and the release of ^{135}Xe as a result of ^{135}I decay are at equilibrium. At equilibrium the amount of ^{135}I being released from the fuel and plating out is equal to that decaying to ^{135}Xe . When the reactor is scrammed, the production and release of ^{135}Xe and ^{135}I from the UO_2 essentially stops, and the ^{135}Xe measured after scram is a result of the decay of the plated out ^{135}I . Thus, by measuring the release of ^{135}Xe after scram, the equilibrium ^{135}I release rate can be determined. The ^{135}I release data were acquired using this technique at the end of the period during which the Xe and Kr gas measurements were conducted.

The ^{131}I and ^{133}I release measurements were made on April 25, 1980, following a reactor shutdown on April 17, 1980. The fuel rod power history for the operating period prior to shutdown is shown in Figure 5. The burnup at the end of the period was ~ 5000 MWd/t. The reactor had been shutdown from January 7, 1980, until the beginning of the period shown in Figure 5, thus the ^{131}I and ^{133}I inventory was essentially zero at the beginning of the period.

The ^{131}I and ^{133}I gap inventories were determined by measuring their decay products, ^{131}Xe and ^{133}Xe , following shutdown. The measurements were made with the following procedure: Approximately four days after reactor shutdown the rods were flushed with He to remove the Xe

from the fuel-cladding gap and plenum region and the in-pile fast-action valves (Figure 3) were closed. The iodine that had plated out in the gap and plenum region continued to decay to Xe, thus the Xe inventory in the gap region slowly increased. The Xe inventory now, however, was due solely to decay of the plated-out iodine (diffusion is essentially zero at zero power, low temperature conditions); this permits the inventory of iodine which is decaying to be determined by measuring the Xe. Thus, at about four days following the first flushing the rods were again flushed and the Xe content was measured. The measured Xe content was then used to determine the iodine gap inventory at shutdown using standard radioactive decay equations; Appendix A contains a description of the calculation procedure.

3. EXPERIMENT RESULTS

The experiment results, in the form of isotopic release rate data, release-to-birth ratios, and release fractions are presented in the following sections. Details of the determination of the release rate from the gamma spectrometer data and details of the birth calculations are contained in Appendices A and B.

3.1 Noble Gases

The release rate of the noble gas isotopes from the fuel is determined using

$$R = \frac{fAT_p e^{\lambda t_d}}{T_g \epsilon BV_p T_p \lambda} \quad (1)$$

where

- R = release rate (atoms/s)
- f = flow rate (cm³/s at STP)
- A = area of gamma peak in spectrum (counts)
- T_p = temperature of gas at detector location (K)
- P = standard pressure (0.1013 MPa)
- T_g = gamma spectrum live time (s)
- ε = detector geometry efficiency
- B = gamma ray abundance (number of gamma's emitted/decay)

TABLE 2. MEASURED RELEASE RATES OF XENON

| | ^{137}Xe | ^{138}Xe | ^{135}Xe | ^{135}Xe | ^{133}Xe | Isotope | | |
|---------|-------------------------------------|--------------------------------|-------------------------------|--|------------------------------|-----------|-----------------------------------|--------------------|
| | 3.84 min 3.01 E-3 455.5 | 14.13 min 8.17 E-4 258.3 | 15.6 min 7.40 E-4 526.6 | 9.09 h 2.12 E-5 ^b 249.8 | 5.25 d 1.53 E-6 81.0 | Half-Life | Decay Constant (s ⁻¹) | Gamma Energy (KeV) |
| | Release Rate ^a (atoms/s) | | | | Flow (cm ³ /s) | Rod No. | Spectrum Number | |
| 14 | 1.78 E9 | 2.49 E9 | 7.08 E8 | 9.34 E9 | -- | 9.0 | 4 | 20 |
| | 1.94 E9 | 2.75 E9 | 8.15 E8 | 9.28 E9 | -- | 8.7 | 4 | 21 |
| | 2.50 E9 | 3.23 E9 | 8.26 E8 | 6.68 E9 | -- | 15.3 | 4 | 22 |
| | 2.45 E9 | 3.21 E9 | 9.28 E8 | 6.34 E9 | -- | 15.3 | 4 | 23 |
| | 2.58 E9 | 3.32 E9 | 8.26 E8 | 8.26 E9 | -- | 15.3 | 4 | 11 |
| | 2.56 E9 | 3.37 E9 | 8.77 E8 | 6.62 E9 | -- | 15.3 | 4 | 12 |
| | 2.51 E9 | 3.35 E9 | 8.49 E8 | 6.51 E9 | -- | 15.3 | 4 | 13 |
| | 2.51 E9 | 3.31 E9 | 8.66 E8 | 6.34 E9 | -- | 15.3 | 4 | 14 |
| | 2.86 E9 | 3.48 E9 | 7.64 E8 | 6.17 E9 | -- | 24.2 | 4 | 24 |
| | 2.75 E9 | 3.34 E9 | 8.43 E8 | 4.64 E9 | -- | 24.2 | 4 | 25 |
| | 3.06 E9 | 3.44 E9 | 8.15 E8 | 4.64 E9 | -- | 32.8 | 4 | 26 |
| | 2.94 E9 | 3.03 E9 | 7.08 E8 | 4.42 E9 | -- | 32.8 | 4 | 27 |
| | 3.02 E9 | 3.14 E9 | 8.49 E8 | -- | -- | 51.7 | 4 | 28 |
| | 3.05 E9 | 2.99 E9 | 8.43 E8 | -- | -- | 51.7 | 4 | 29 |
| 7.92 E8 | 1.02 E9 | 5.25 E8 | 4.01 E9 | 1.72 E10 | 14.5 | 2 | 15 | |
| 7.87 E8 | 1.01 E9 | 5.25 E8 | 3.68 E9 | 1.32 E10 | 14.5 | 2 | 16 | |
| 7.75 E8 | 1.02 E9 | 4.97 E8 | 4.36 E9 | 1.69 E10 | 14.5 | 2 | 17 | |
| 7.75 E8 | 1.05 E9 | 4.87 E8 | 5.61 E9 | 1.99 E10 | 14.5 | 2 | 18 | |

a. NOTATION: m.mm E n = m.mm x 10ⁿ.

b. Corrected for neutron capture.

TABLE 3. MEASURED RELEASE RATES OF KRYPTON

| | ^{89}Kr 3.16 min 3.66 E-3 220.9 | ^{87}Kr 1.27 h 1.51 E-4 402.6 | ^{88}Kr 2.84 h 6.78 E-5 196.3 | $^{85\text{m}}\text{Kr}$ 4.48 h 2.12 E-5 151.2 | Isotope Half-Life Decay Constant (s^{-1}) Gamma Energy (KeV) | | |
|----|---|---|---|---|--|---------|--------------------|
| | Release Rate ^a (atoms/s) | | | | Flw (cm ³ /s) | Rod No. | Spectrum Number |
| 15 | 1.35 E9 | 1.85 E9 | -- | 2.10 E9 | 9.0 | 4 | 20 |
| | 1.39 E9 | 1.92 E9 | 3.95 E9 | 2.10 E9 | 8.7 | 4 | 21 |
| | 1.91 E9 | -- | -- | 1.92 E9 | 15.3 | 4 | 22 |
| | 1.92 E9 | -- | -- | -- | 15.3 | 4 | 23 |
| | 1.92 E9 | -- | -- | 1.98 E9 | 15.3 | 4 | 11 |
| | 1.88 E9 | -- | -- | 2.39 E9 | 15.3 | 4 | 12 |
| | 1.89 E9 | -- | -- | 2.16 E9 | 15.3 | 4 | 13 |
| | 1.90 E9 | -- | -- | 1.92 E9 | 15.3 | 4 | 14 |
| | 2.19 E9 | -- | -- | 1.98 E9 | 24.2 | 4 | 24 |
| | 2.14 E9 | -- | -- | -- | 24.2 | 4 | 25 |
| | 2.46 E9 | -- | -- | -- | 32.8 | 4 | 26 |
| | 2.55 E9 | -- | -- | -- | 32.8 | 4 | 27 |
| | 2.88 E9 | -- | -- | -- | 51.7 | 4 | 28 |
| | 2.85 E9 | -- | -- | -- | 51.7 | 4 | 29 |
| | 5.35 E8 | 7.27 E8 | -- | 7.64 E8 | 14.5 | 2 | 15 |
| | 5.83 E8 | 7.32 E8 | -- | 8.38 E8 | 14.5 | 2 | 16 |
| | 5.31 E8 | 7.79 E8 | 1.42 E9 | 1.98 E8 | 14.5 | 2 | 17 |
| | 5.30 E8 | 8.67 E8 | -- | 9.40 E8 | 14.5 | 2 | 18 |

a. Notation: m.mm E n = m.mm x 10ⁿ

- V_p = volume of pipe viewed by detector (cm^3)
 T = standard temperature (273 K)
 P_p = pressure of gas in pipe at detector (MPa)
 λ = decay constant of isotope (s^{-1})
 t_d = delay time of gas from fuel rod to detector (s)

Tables 2 and 3 present the measured release rates for the noble gases Xe and Kr along with the spectrum number and flow rate for each measurement. The uncertainty in the individual measurements is +50-20%, based on a typical linear error propagation (see Appendix D).

The release rate measurements at each particular flow rate are very consistent, the standard deviation being less than 10% of the average release rate. The measurements are also repeatable, as evidenced by the agreement between the release rates in spectrum number 22 and 23 as compared to those in spectra 11 to 14, which were made ~24 hours apart.

The release rates for Rod 4 (diametral gap of 0.10 mm) are consistently higher than those for Rod 2 (diametral gap of 0.23 mm). The difference is believed to be the result of possible leakage through Rod 2 when Rod 4 is used due to the high pressure necessary to establish flow in Rod 4. The Rod 2 data is believed to be most accurate.

The production, or birth, rates of the noble gas isotopes were calculated with the ORIGEN¹³ isotope generation and depletion code. Appendix B provides a summary of the ORIGEN calculations. The calculated birth rates were combined with the average measured release rates for flow rates between 0.5 and 2.0 L/m (Tables 2 and 3), to determine the release-to-birth (R/B) ratios shown in Table 4 for each of the isotopes. The R/B ratio is equivalent to the steady state fractional release rate at equilibrium conditions.

TABLE 4. AVERAGE RELEASE TO BIRTH RATIOS FOR ROD 4
AT 25.5 W/GM AND ROD 2 AT 23.6 W/GM

| <u>Isotope</u> | <u>Rod 4 R/B</u> | <u>Rod 2 R/B</u> |
|----------------|----------------------|----------------------|
| 137Xe | 4.8 E-5 | 1.6 E-5 |
| 138Xe | 5.7 E-5 | 2.0 E-5 |
| 135mXe | 8.5 E-5 | 4.7 E-5 |
| 135Xe | 2.2 E-4 | 1.2 E-4 |
| 133Xe | -- | 3.3 E-4 |
| 89Kr | 4.9 E-5 | 1.5 E-5 |
| 87Kr | 9.1 E-5 | 3.8 E-5 |
| 88Kr | 1.3 E-4 | 4.7 E-5 |
| 85mKr | 1.9 E-4 | 8.0 E-5 |

3.2 Iodine Release

The release rate of iodine cannot be measured directly as iodine, unlike the noble gases, plates out on the cladding inside surface and the gas system piping and is not carried to the FPMS detector location by the He gas stream. However, the iodine release rate can be measured indirectly by allowing the iodine to decay to Xe, which is carried to the detector by the He gas stream. The basic technique was described in Section 2.

The release rate of ^{135}I for Rod 4 was determined by measuring the ^{135}Xe daughter for three days prior to a reactor scram and for ~ 20 hours following the scram. Figure 6 shows the release rate of ^{135}Xe normalized to the release rate at equilibrium (prior to scram) for the period before and after scram. The ^{135}Xe release rate after scram drops off corresponding to the 6.6 hour half life of ^{135}I indicating that essentially all of the ^{135}Xe being measured after scram is due to plated out ^{135}I . Extrapolation of the decay line to the time of scram permits the steady state release rate of ^{135}I to be determined. Figure 6 shows that 52% of the ^{135}Xe being measured prior to scram is due to the decay of plated out ^{135}I ; thus the steady state ^{135}I release rate is 2.30×10^9 atoms/s resulting in a R/B of 4.2×10^{-5} for Rod 2.

The ^{131}I half-life is 8.01 days and thus a steady operating period of ~ 35 days is required to get to $> 95\%$ of equilibrium conditions. Such an irradiation period was not possible during the present tests and thus the steady state equilibrium R/B ratio could not be measured. However, the release fraction, defined as the fraction of non-decayed iodine residing in the fuel-cladding gap and plenum region, can be determined. The release fractions for ^{131}I and ^{133}I were determined using the measured gap inventory as detailed in Section 2.2 and Appendix A and the ORIGEN calculated total rod inventory. The measured release fractions were 2.3×10^{-4} for ^{131}I and 1.5×10^{-3} for ^{133}I . The measurement uncertainty in the release fractions is $\pm 30\%$. However, the release fraction for ^{133}I seems high by a factor of about 10 as discussed further in Section 4.

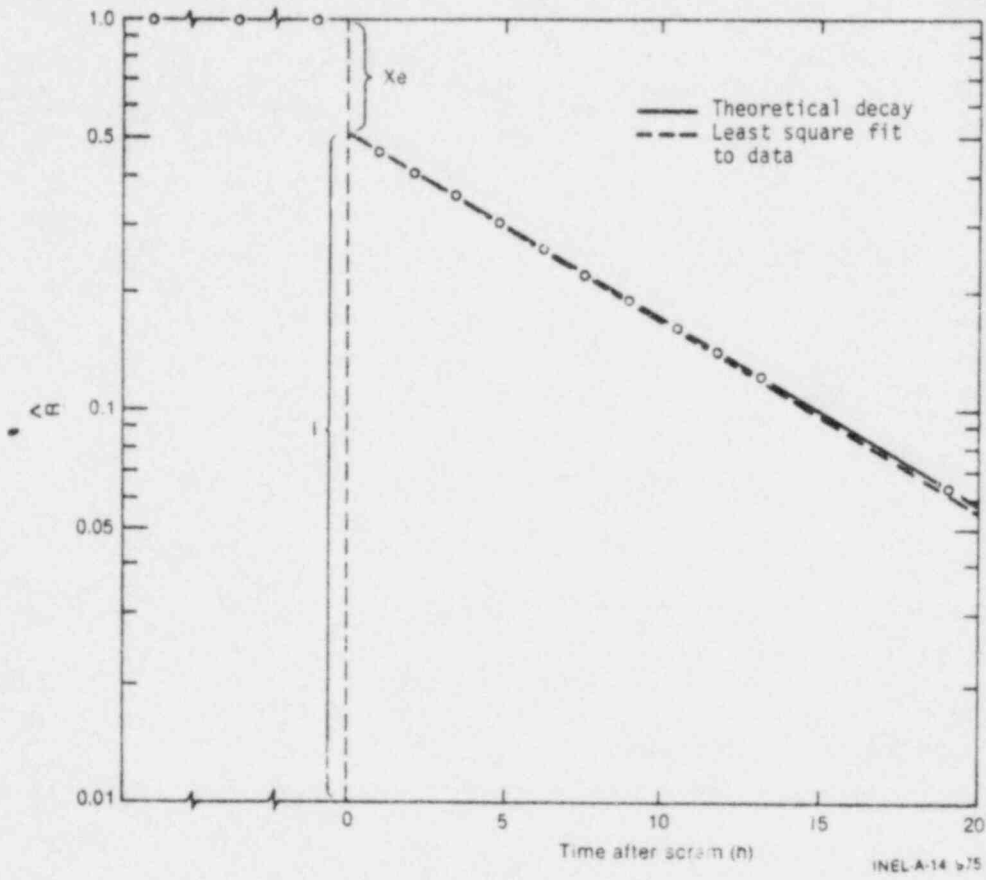


Figure 6. Normalized ^{135}Xe release rate (\bar{R}) as a function of time for three days prior to scram and following scram indicating ^{135}I release rate is 52% of ^{135}Xe release rate.

4. DISCUSSION OF RELEASE MECHANISMS

Fission gases are released from the fuel into the fuel cladding gap by three processes: (1) knockout, in which an energetic fission fragment collides with a previously formed fission gas atom knocking it out of the fuel matrix; (2) recoil, in which the fission gases formed during fission recoil from the fissioning atom and are ejected from the fuel; and (3) diffusion, in which the fission gases diffuse through the fuel matrix until reaching the open porosity in the fuel and escaping. Olander¹⁴ has derived a mechanistic expression for the fractional release rate (R/B) of short lived fission products due to recoil and knockout processes:

$$f_i = \frac{R_i}{B_i} = \frac{\eta_{rec}}{4} \frac{S_g}{V} \mu_{ff} + \frac{1}{\lambda_i} \frac{S_T \alpha_U \dot{F} \mu_{ff}}{4V N_U} \quad (2)$$

where

- η_{rec} = the fraction of direct recoils that are not embedded in other surfaces after ejection from the solid
- S_g = the geometrical surface area of the specimens
- V = the specimen volume
- μ_{ff} = fission fragment range
- λ_i = decay constant
- S_T = the total surface area of the specimens
- α_U = knockout yield
- \dot{F} = fissions $\text{cm}^{-3} \text{ s}^{-1}$
- N_U = density of uranium atoms in the solid.

The first expression on the right hand side of equation (2) is the recoil contribution and the second term the knockout contribution. Recoil and knockout release are believed¹⁴ to dominate the release of fission gases during irradiation at temperatures below 1000 K and at fuel

temperatures > 1000 K the diffusion process becomes significant. Classical diffusion theory, when applied to fission gas release from UO_2 predicts that for an effective sphere size a

$$R/B = \frac{3}{a} \sqrt{\frac{D}{\lambda}} \quad (3)$$

for $(a^2\lambda/D)^{1/2} \gg 1$ where D is the diffusion coefficient.

Obviously, many parameters affect the release process, most of which are not easily measurable: however, the dependence of the R/B on the decay constant λ is measurable and thus a convenient tool for estimating the relative contribution of each release process. The slope of the R/B versus λ curve should indicate which release mechanism is dominating. A slope of zero would correspond to recoil release, a slope of -1 to knockout release, and a slope of -1/2 to diffusion release. Figure 7 shows the Rod 2 average R/B ratios (from Table 6) plotted as a function of decay constant λ . The slope of the least-square-fit-straight line for the data is -0.4, indicating that a combination of release mechanisms are contributing to the total release with no single mechanism dominating. This is not surprising as the temperature of the fuel during the tests ranged from ~ 650 K in the outer edges of the pellets up to ~ 1350 K at the center, which overlaps the upper end of the recoil/knockout-dominant temperature region and the lower end of the diffusion-dominant region. However, the closeness of the measured slope to that of the slope expected for diffusion indicates that the release can be described in terms of diffusion.

Based on the above conclusion the measured ^{133}I release fraction appears to be about a factor of 10 high. The ^{131}I and ^{135}I isotopes follow the expected $\lambda^{-1/2}$ behavior, as shown in Figure 7 while the ^{133}I value of 1.5×10^{-3} is a factor of 10 higher than would be expected for a half-life of 20 h ($\ln \lambda = -11.6$). Thus the ^{133}I release fraction is believed to be erroneously high; further tests are being conducted to resolve the problem.

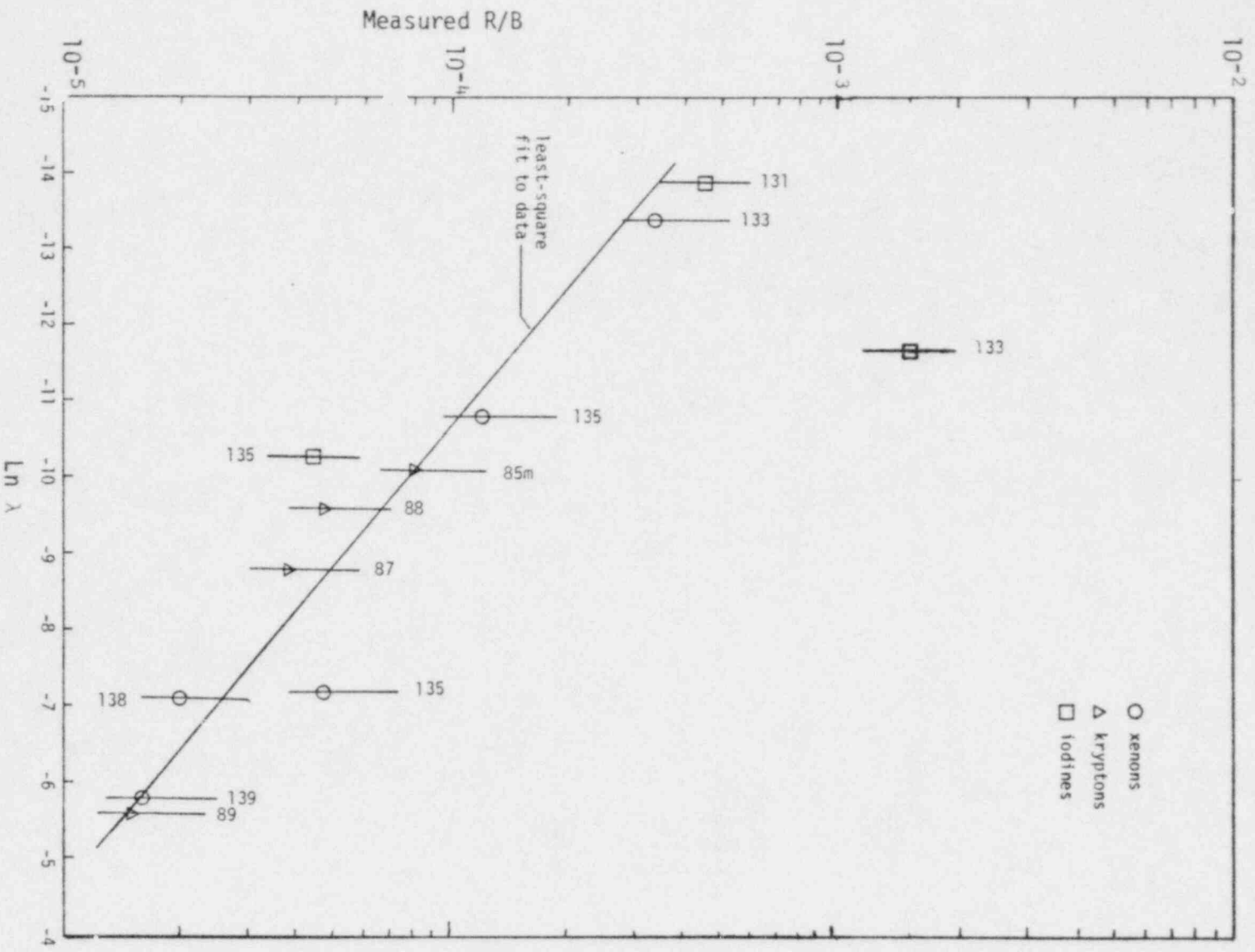


Figure 7. IFA-430 measured release-to-birth ratio (R/B) as a function of decay constant. The slope of the least-square-fit line (excluding the ^{133}I) is -0.4, indicating that the R/B could be described by a diffusion model.

5. COMPARISON WITH RELEASE MODELS

Two models for predicting fission gas release have been chosen for comparison with the data based on their applicability to short lived fission gas release; (a) the American Nuclear Society (ANS) proposed standard method (5.4) for calculating the release of fission products from oxide fuel³ and (b) the diffusion model of Friskney and Turnbull.^{8,16}

A brief summary of each model and a comparison with the IFA-430 fission gas release data are presented in the following two sections.

5.1 ANS 5.4

The ANS 5.4 proposed standard method for calculating the release of fission products from oxide fuel applies to steady-state conditions. It is intended to provide the fractional release and thus the inventory of volatile fission products that could be available for release from a fuel rod if the cladding were breached. The model is intended to give best-estimate predictions of release fractions but is empirical in nature and should not be interpreted as a detailed physical description of the release mechanism.

The fractional release as used in the ANS standard is defined as the fraction of non-decayed inventory that resides in the gap (i.e., free volume outside of the fuel pellet but inside of the fuel rod cladding). The standard consists of four models, one each for high temperature and low temperature release of long-lived (> 1 year) and short-lived (< 1 year) isotopes. The high and low temperature ranges are not defined in the standard but rather the release is calculated using both the high and low temperature models and the larger of the two releases is taken as the result.

The high temperature release fraction, F, for short lived isotopes at constant temperature and power is

$$F = \frac{3}{1 - \exp(-\mu\tau)} \frac{1}{\sqrt{\mu}} [\operatorname{erf}(\sqrt{\mu\tau}) - 2\sqrt{\mu}/\pi \exp(-\mu\tau)] - \frac{1 - (1 + \mu\tau)\exp(-\mu\tau)}{\mu}, \quad (\tau \leq 0.1) \quad (4)$$

and

$$F = 3 \frac{1}{\sqrt{\mu}} \coth(\sqrt{\mu}) - \frac{1}{\mu} - \frac{6\mu}{\exp(\mu\tau) - 1} \times \sum_{n=1}^{\infty} \frac{1 - \exp(-n^2\pi^2\tau)}{n^2\pi^2(n^2\pi^2 + \mu)}, \quad (\tau > 0.1) \quad (5)$$

where

$$D' = [D_0/a^2) \exp(-Q/RT)] \times 100^{\text{Bu}/28,000}$$

$$D_0/a^2 = 0.61 \text{ sec}^{-1} \text{ where the notation } D_0/a^2 \text{ is retained for consistency with published references}$$

$$Q = 72,3000 \text{ cal/mol}$$

$$\mu = \lambda/D'$$

$$\tau = D't$$

$$\lambda = \text{decay constant (s}^{-1}\text{)}$$

$$t = \text{time (s) during the constant-temperature and constant power irradiation period}$$

$$T = \text{fuel temperature (K)}$$

$$\text{Bu} = \text{total accumulated burnup (MWd/t) including all prior operating periods.}$$

For low temperature release of short lived isotopes

$$F = (1/\tau) [10^{-7} \sqrt{\tau} + 1.6 \times 10^{-12} P] \quad (6)$$

where P is the specific power (megawatts per metric ton of heavy metal), and where for conservatism, P corresponds to the maximum power level during the last two half lives of operation.

When calculating the release fraction for ^{133}Xe and ^{135}Xe , ANS 5.4 recommends that the fractional release of the precursors (^{133}I and ^{135}I , respectively) be added to the release of ^{133}Xe and ^{135}Xe . The release of iodine is calculated using the same models as for the noble gases except that the diffusion coefficient, D', for iodine is seven times that of its xenon daughter.

The ANS 5.4 proposed standard has been incorporated as a subroutine in the FRAPCON-2¹⁵ steady-state fuel rod behavior code, and was used to calculate the fission gas release fraction for the isotopes measured with the IFA-430 system. The controlling factors of fission gas release in the ANS 5.4 model are fuel temperature, burnup, and rod power. The IFA-430 FRAPCON-2 fuel rod model was set up such that the calculated fuel centerline temperature, burnup, and rod power corresponded to the IFA-430 fuel conditions at the time of the fission gas release measurements. Because fuel centerline thermocouple holes cannot be restricted to a single axial segment in FRAPCON-2, the model was first set up with a thermocouple hole extending the length of the fuel stack and optimized to match the measured temperatures. The thermocouple hole was then removed from the model so that the fuel temperatures would be representative of the major portion of the IFA-430 fuel, (~94% of the IFA-430 fuel stack does not have a thermocouple hole at the center) and the fission product release fraction calculated with the ANS 5.4 subroutine. Figure 8 shows the measured and FRAPCON-2^a calculated fuel centerline temperature with and

a. FRAPCON-2 Configuration Control Number H010585B.

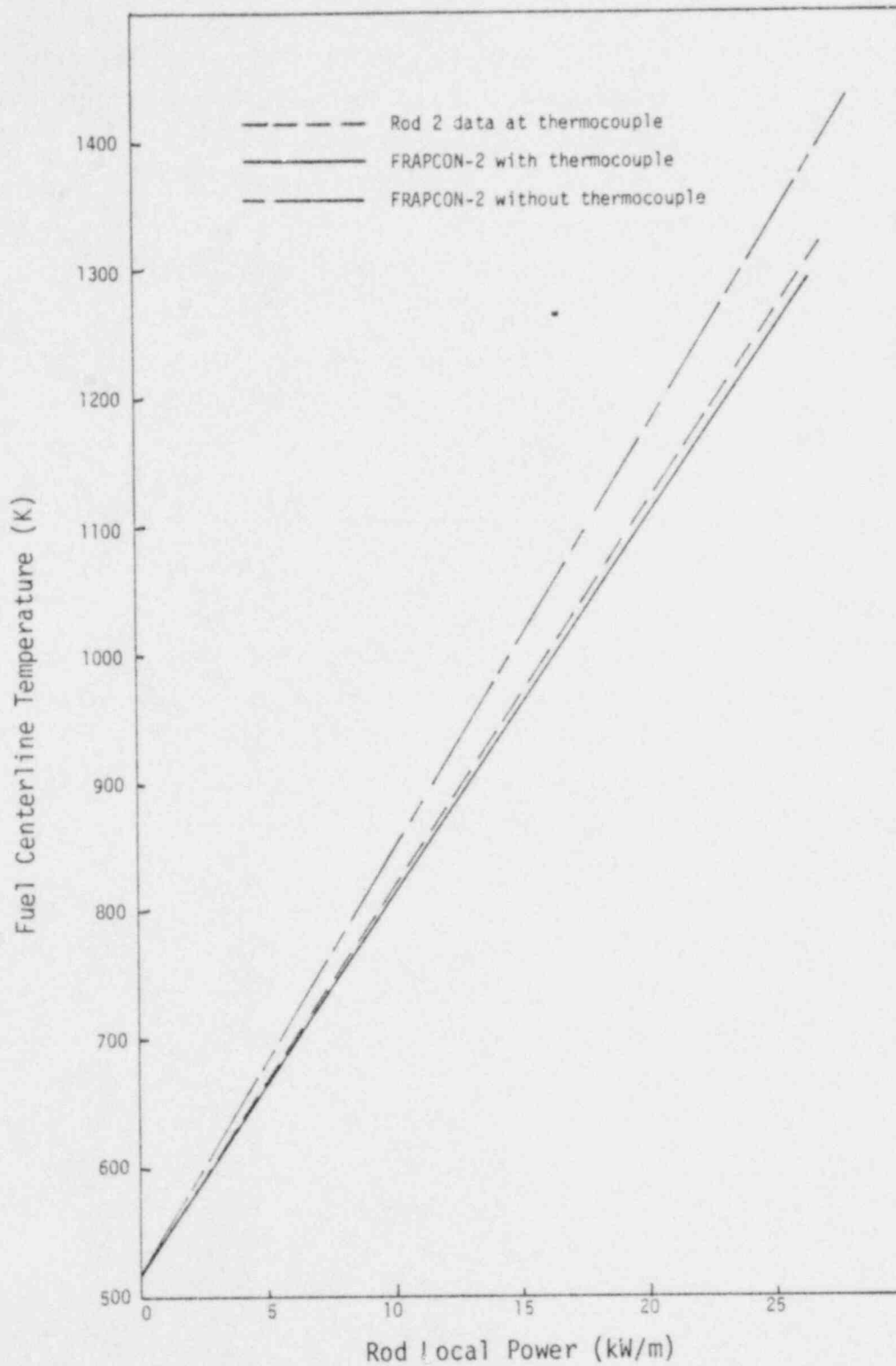


Figure 8. FRAPCON-2 calculated fuel centerline temperature, with and without a fuel thermocouple hole included in the model, and the IFA-430 Rod 2 centerline temperature as a function of local rod power.

without a thermocouple hole in the fuel model as a function of local power. Figures 9 and 10 show the ANS 5.4 calculated release fractions for the noble gases compared to the measured data.

The ^{135}Xe and ^{133}Xe ANS 5.4 calculated release fractions are within the uncertainty band of the data (Figure 9) when the iodine precursor is included; however, the calculated release fractions of the shorter lived isotopes of Xe are lower than the measured release fractions by a factor of ~ 2 . The ANS 5.4 calculated release fractions for Kr are all lower than those measured by factors of about 2 to 4.

To estimate the expected order of magnitude of the release fraction for a successfully terminated LOC type accident the FRAPCON-2 peak fuel centerline temperature was set to ~ 1450 K and the ANS 5.4 model used to calculate the release fraction. The results, shown in Figures 11 and 12, indicate that the expected release fraction is generally on the order of 10^{-4} to 10^{-3} for Xe and 10^{-5} to 10^{-4} for Kr.

The ANS 5.4 calculated release fractions for iodine are compared with the measured release fractions in Figure 13. The details of the release fraction calculations are given in Appendix A. The ^{131}I calculated release fraction is within the uncertainty band of the measured data and the calculated ^{135}I release fraction is higher by a factor of ~ 2 .

Figure 14 presents a summary of the ANS 5.4 predicted versus measured release fractions for the noble gases and iodines; the ANS 5.4 model is underpredicting the short half-lived isotopes of Xe and Kr but agrees fairly well with the medium half-lived (> few hours) isotopes.

5.2 Diffusion Model

Of the three postulated mechanisms for release of fission products, recoil, knockout and diffusion, it has generally been believed¹⁴ that at temperatures below ~ 1000 K recoil and knockout were the dominating mechanisms. However, recent experiments¹⁶ performed in the United Kingdom have shown that at temperatures as low as 500 K the kinetics of

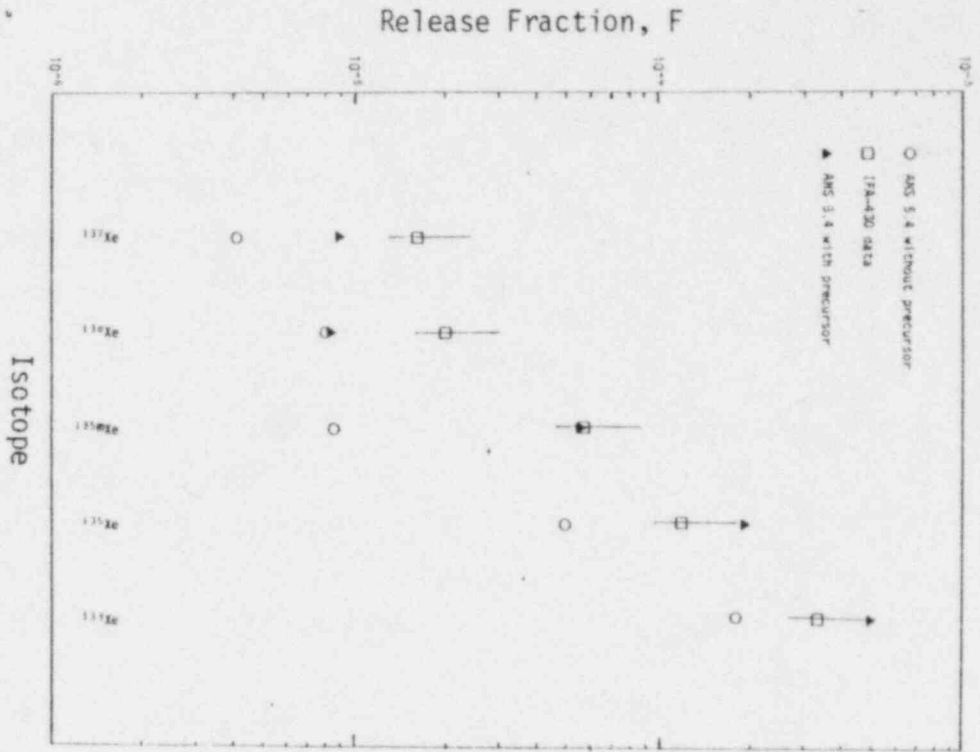


Figure 9. ANS 5.4 calculated release fractions, F , compared with IFA-430 measured release fractions for xenon isotopes.

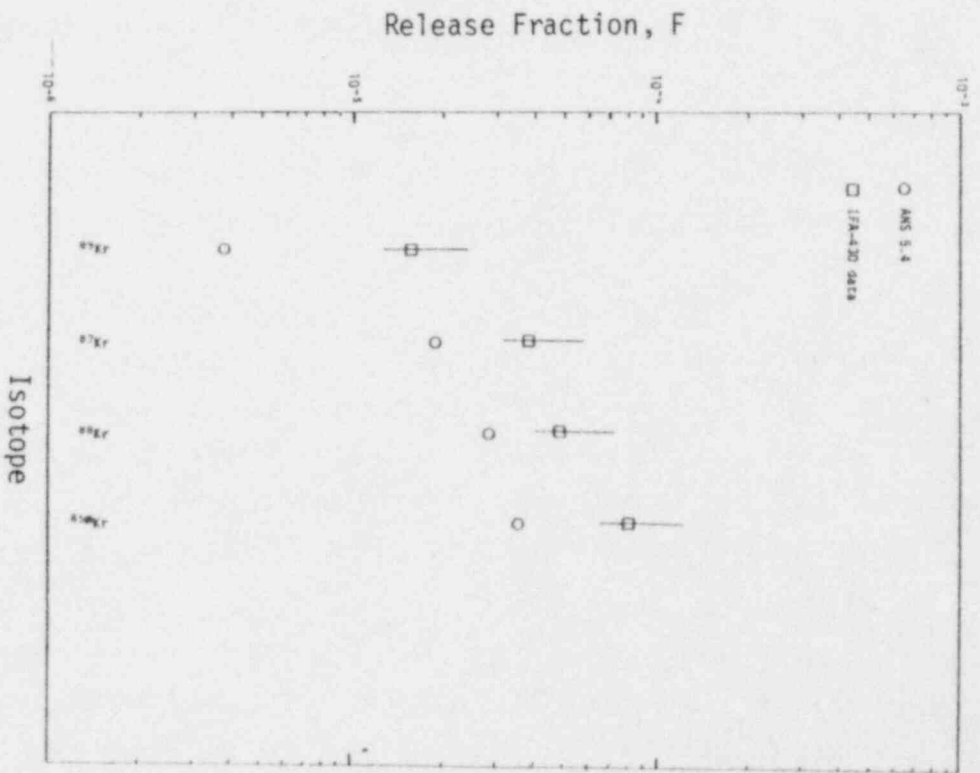


Figure 10. ANS 5.4 calculated release fractions, F , compared with IFA-430 measured release fractions for krypton isotopes.

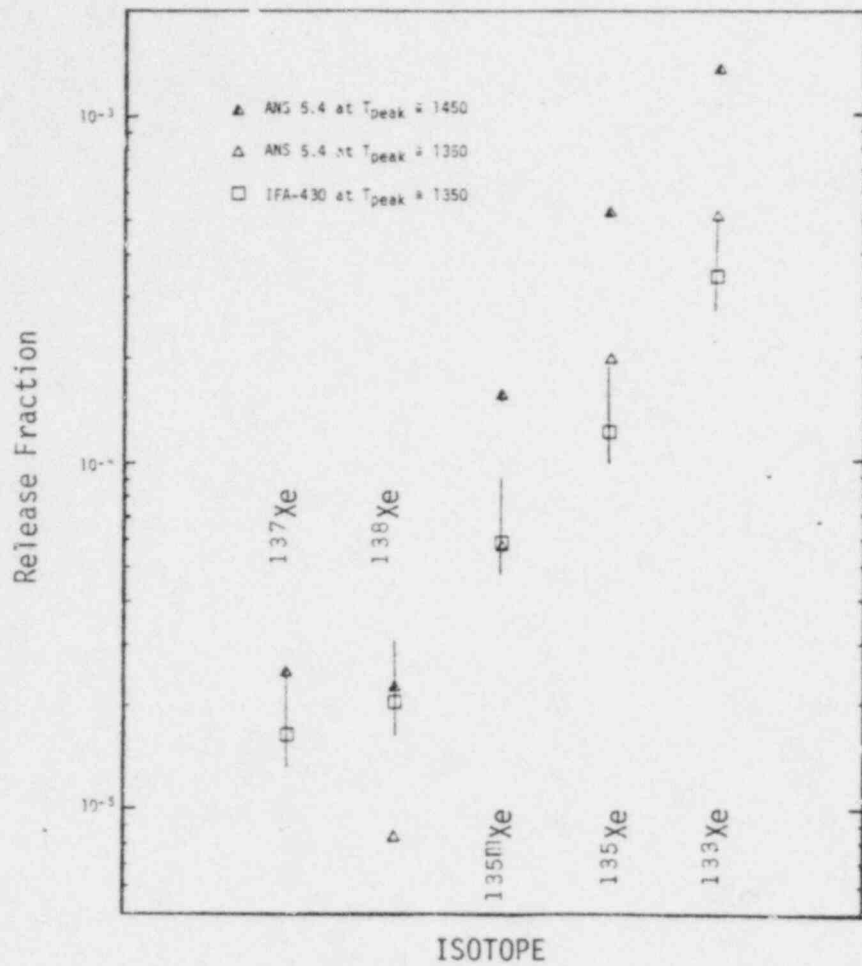


Figure 11. ANS 5.4 calculated release fraction for peak fuel centerline temperatures of about 1350 and 1450 K compared with IFA-430 measured release fraction at fuel peak centerline temperature of about 1350 K.

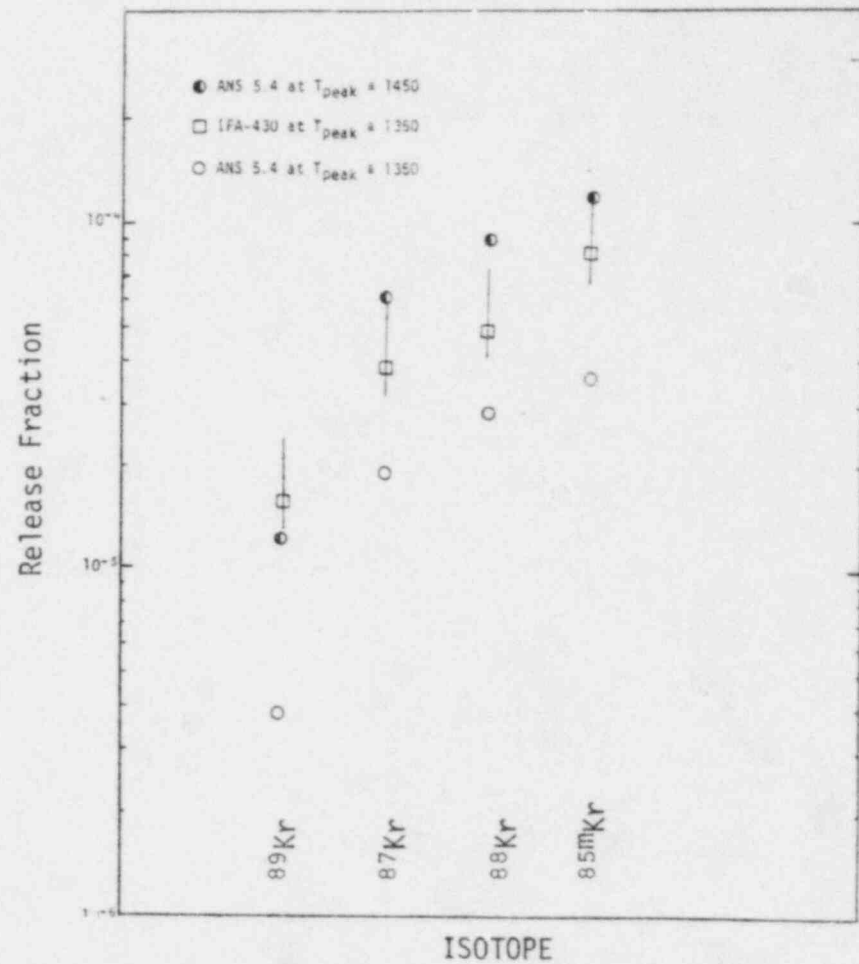


Figure 12. ANS 5.4 calculated release fraction for peak fuel centerline temperatures of about 1350 and 1450 K compared with measured release fraction at about 1350 K.

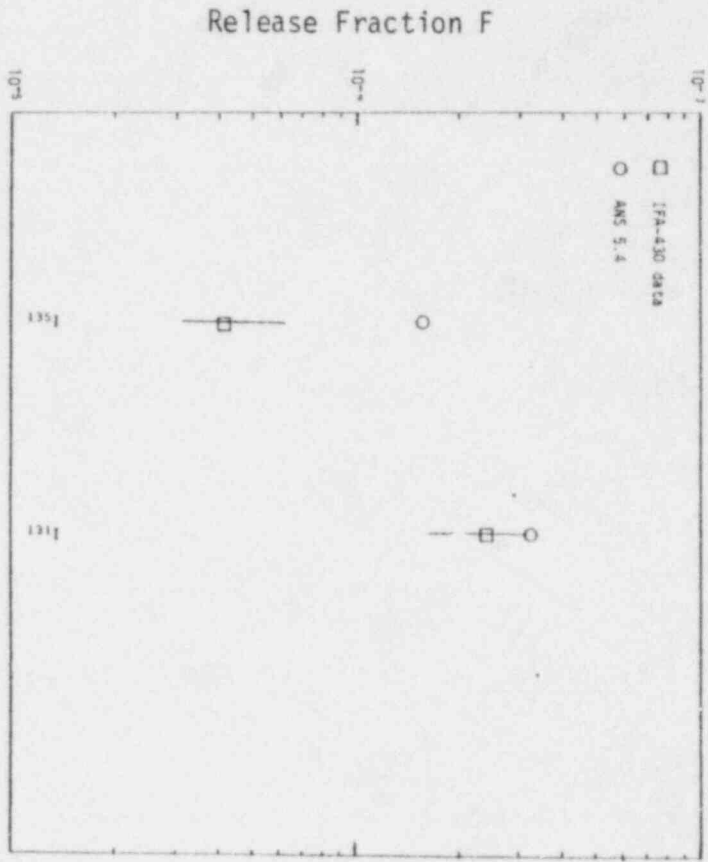


Figure 13. ANS 5.4 calculated release fractions and IFA-430 measured release fractions for iodine.

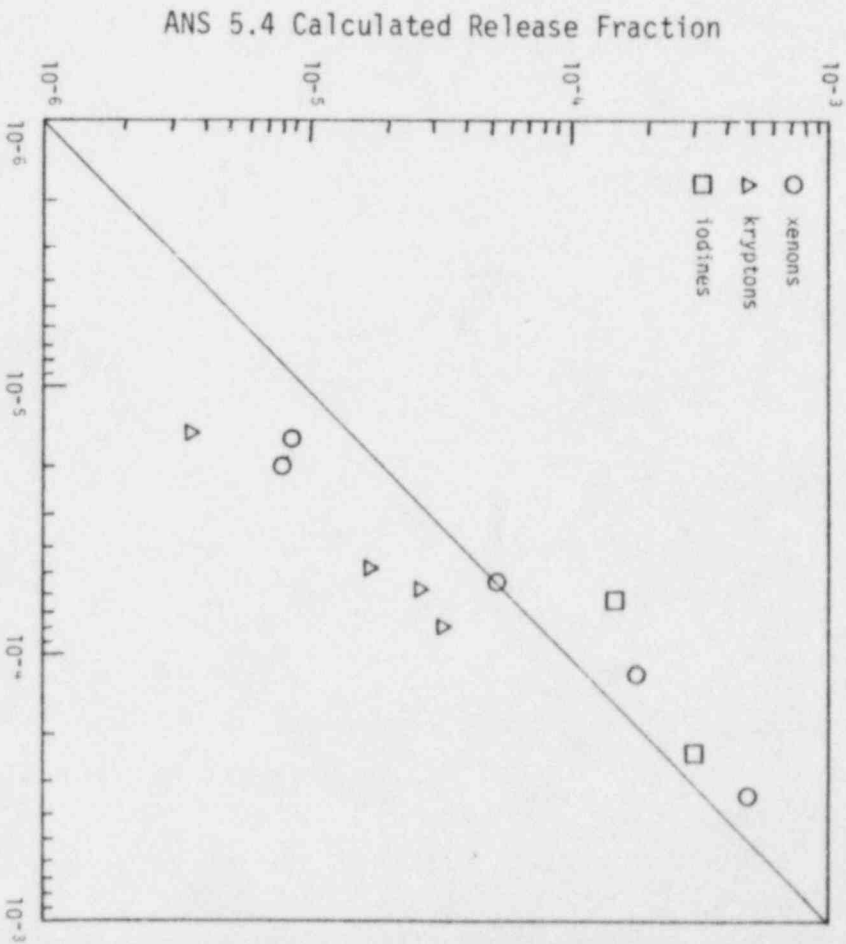


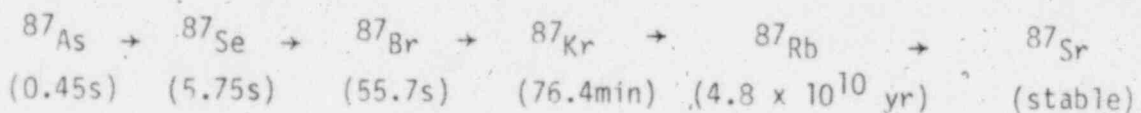
Figure 14. ANS 5.4 predicted release fraction versus IFA-430 measured release fraction.

release can be described in terms of diffusion. As shown in Section 4, the relationship between the release-to-birth ratio (R/B) and decay constant for the IFA-430 data tend to support this. Even though the average bulk temperature of the IFA-430 fuel was ~850 K, the measured results show that the slope of the R/B versus λ curve is -0.4, close to the -0.5 slope corresponding to diffusion release. Thus, it appears that the release of fission gases from the IFA-430 fuel should be describable with a diffusion model.

The general diffusion model describes R/B as:

$$R/B = \left(\frac{S}{V}\right) \sqrt{D/\lambda} \quad (7)$$

The equation applies to conditions of radioactive equilibrium for (R/B) < 0.1 where, S/V) is the surface to volume ratio and D is the effective diffusion coefficient. However, because the isotopes of Xe and Kr result primarily from the decay of shorter lived precursors rather than as a direct product of fission; the behavior, i.e. diffusion, of the precursors has to be taken into account. As an example, the decay chain which includes ⁸⁷Kr is



where the half-life is given in parentheses. In describing the diffusion of ⁸⁷Kr the isotopes ⁸⁷As and ⁸⁷Se are too short lived to influence appreciably the release kinetics; however, ⁸⁷Br has a long enough half life and high enough diffusion coefficient (~200 times that of Kr)¹⁶ to affect the kinetics of ⁸⁷Kr release. The influence of precursors is different for each decay chain and must be evaluated for each case. In the case of Xe the only important precursor is iodine, which has a diffusion coefficient almost identical to Xe.^{8,9} Thus the value for D in Equation 7 is dependent upon the species and the isotope. An equation which considers the influence of precursors on the R/B has been proposed by Friskney and Speight.¹⁷ with the subscripts 1 and 2 referring to the precursor and daughter respectively, R/B is given as

$$(R/B) = 3 \left[\frac{\text{Coth } y - 1/y}{y(1-y^2/x^2)} + \frac{\text{Coth } x - 1/x}{x(1-x^2/y^2)} \right] \quad (8)$$

where

$$s = 3\left(\frac{V}{S}\right) \sqrt{\frac{\lambda_1}{D_1}} \quad \text{and} \quad y = 3\left(\frac{V}{S}\right) \sqrt{\frac{\lambda_2}{D_2}}$$

However, since it has been determined experimentally^{8,9} that $D_I = D_{Xe}$, $D_{Kr} = (1/2) D_{Xe}$ and $D_{Br} = 200 D_{Kr}$, Equation (8) can be reduced to

$$R/B = \left(\frac{S}{V}\right) \sqrt{\frac{kD}{\lambda}} \quad (9)$$

where λ is that for the noble gas, k is a constant for each parent-daughter relationship, and D is the diffusion coefficient for Xe. Table 5 gives the values of k for several Xe and Kr isotopes.

The diffusion coefficients used in Equation (9) are best described as effective diffusion coefficients since they are dependent on not only temperature but also on the irradiation conditions.¹⁶ An equation for the temperature and power dependent effective diffusion coefficient for Xe has been determined:¹⁶

$$D = 7.6 \times 10^{-6} \exp(-3.5 \times 10^4/T) + 1.41 \times 10^{-18} \varnothing^{1/2} \exp(-1.38 \times 10^4/T) + 2 \times 10^{-30} \varnothing \quad (10)$$

where \varnothing is the mass power rating (W/g) and T is the temperature (K). Figure 15 shows the relationship of D to T for linear heat ratings of 10 and 40 kW/m.

The diffusion model (Equation 9) was used to calculate the R/B for IFA-430 Rod 2. In the model the fuel rod was divided into 12 axial segments of 10 cm length each. Postirradiation examination¹⁷ of fuel

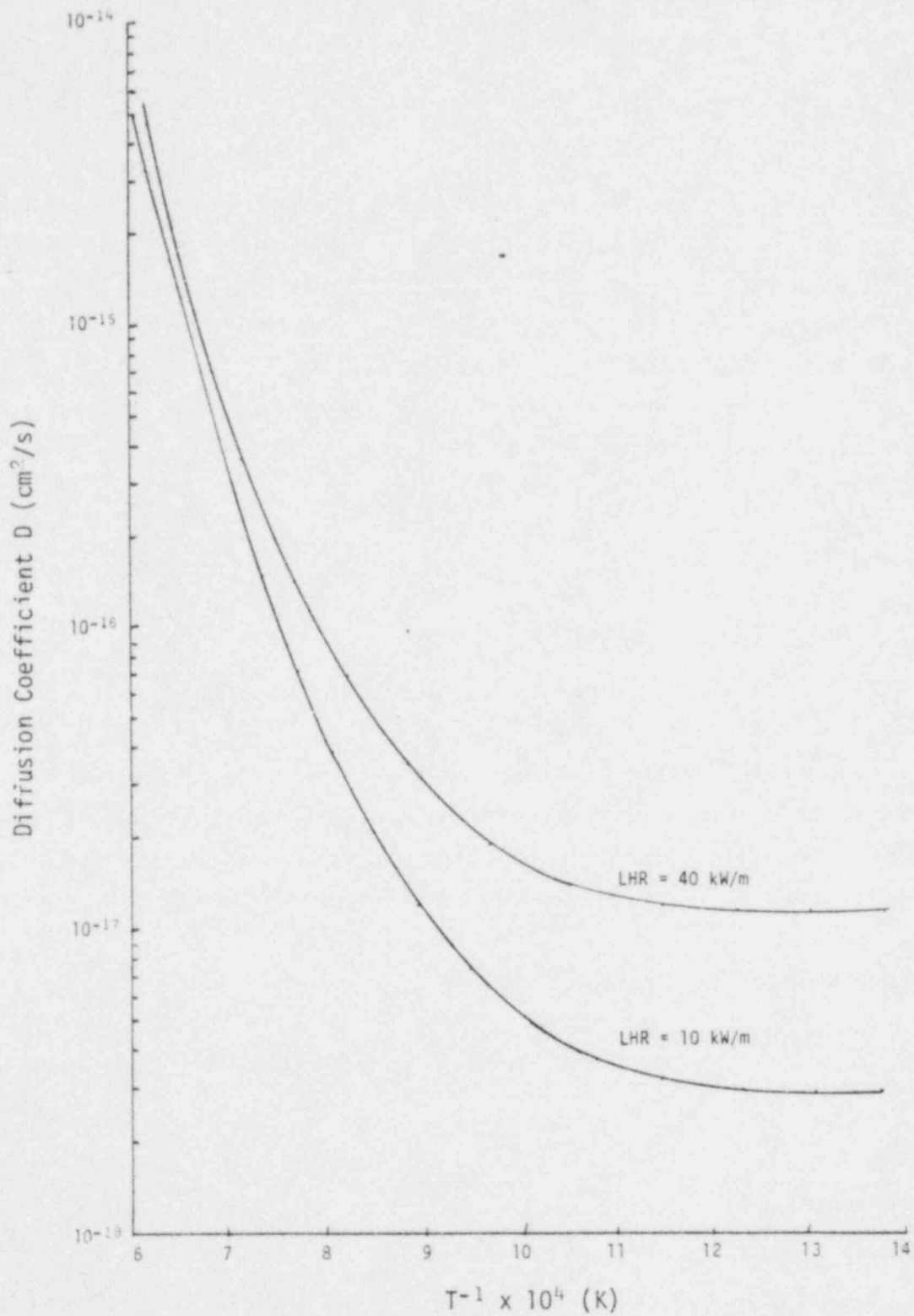


Figure 15. Diffusion coefficient D , calculated with Equation (9), for rod linear heat rates (LHR) of 10 and 40 kW/m as a function of inverse-temperature.

made to the same specification as the IFA-430 fuel and irradiated under similar conditions showed that the pellets had from 4 to 7 radial cracks and no circumferential cracks. Therefore, two cases were examined: (a) assuming the pellets have 7 radial cracks, resulting in a surface area equal to 10 times the geometric surface area and; (b) assuming the pellets had 4 radial cracks resulting in a surface area about 4 times the geometric surface area.

The total release, the summation of all the axial segments, was then divided by B for the whole rod to determine R/B. Figure 16 shows the calculated and measured R/B as a function of λ for Rod 2 with four radial cracks assumed. The calculated R/B are lower than the predicted by about 60%, indicating that the surface area was probably underestimated by $\sqrt{60\%}$. Figure 17 compares the measured and predicted R/B for a surface area of 10 times the geometric surface area corresponding to a pellet with seven radial cracks; the agreement is excellent.

The diffusion model predicts not only the general dependence of R/B on λ , but also the relationship between the different isotopes. For example, the kinks in the R/B versus λ curve (Figure 17) are predicted by the model. This form of agreement is more significant than a general agreement with the magnitude of the release since the magnitude is controlled by the surface to volume ratio and the ratio of the true to geometric surface area. The good prediction of the relative values for release indicates that the model is apparently applying the correct mechanisms to account for precursor effects and element dependent diffusion coefficients.

TABLE 5. PARENT-DAUGHTER CONSTANT k FOR Xe AND Kr ISOTOPES

| Isotope | k |
|--------------------------|-------|
| ^{133}Xe | 1.25 |
| ^{135}Xe | 3.96 |
| ^{138}Xe | 1.014 |
| $^{85\text{m}}\text{Kr}$ | 1.74 |
| ^{88}Kr | 0.71 |
| ^{87}Kr | 1.90 |

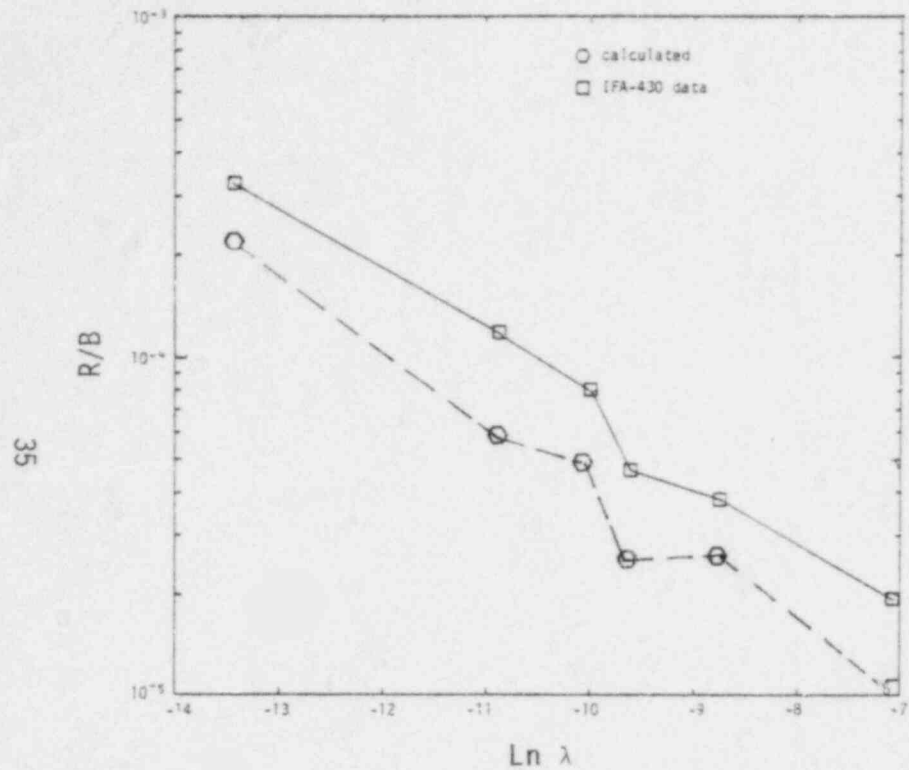


Figure 16. Equation (9) calculated and IFA-430 measured R/B as a function of decay constant. The S/V used in Equation (9) corresponds to a surface area of 4 times the geometric surface area.

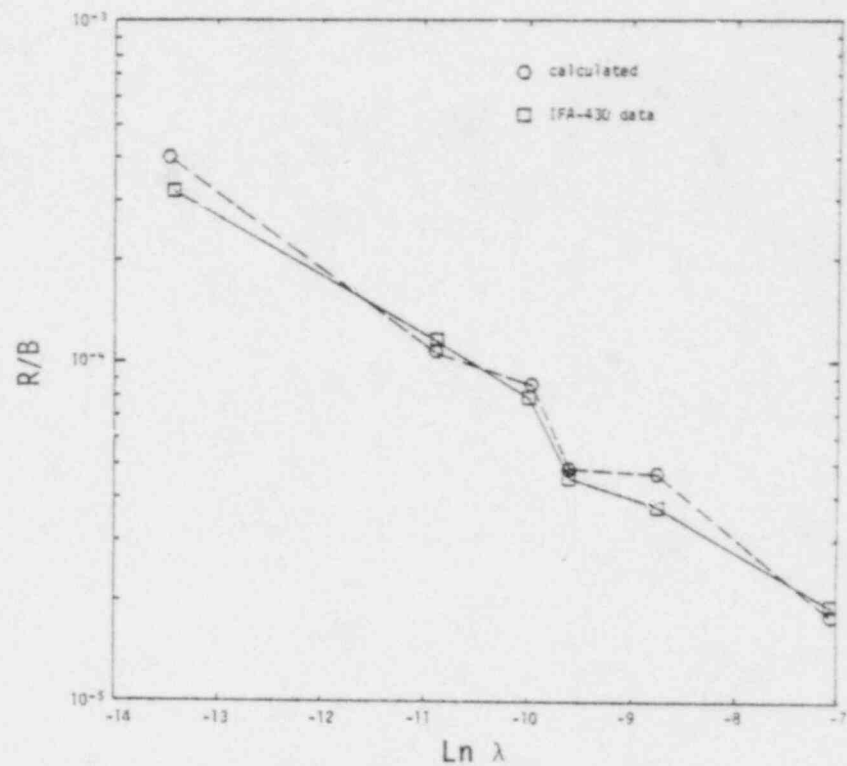


Figure 17. Equation (9) calculated and IFA-430 measured R/B as a function of decay constant. The S/V used in Equation (9) corresponds to a surface area of 10 times the geometric surface area.

6. DISCUSSION AND CONCLUSIONS

The release of fission products from the fuel pellets to the fuel-cladding gap and rod plenum is of concern to reactor safety because the fission products in the gap can affect the thermal behavior of the fuel, may contribute to cladding failure, and are readily available for release should the fuel cladding fail. The Nuclear Regulatory Commission has established regulatory guides which prescribe the assumptions to be invoked when calculating, for safety analysis, the inventory of gaseous and volatile fission products in the fuel-cladding gap and plenum region. To ensure the public safety the regulatory guides are conservative; however, the amount of conservatism is believed¹ to be excessive in some cases. The overconservatism is being addressed by the NRC in an attempt to establish more realistic, while still conservative with respect to public safety, guidelines.

Two areas of concern^{1,2} are the Loss of Coolant (LOC) type accident and the Fuel Handling type accident; in addition, the operational transient (OPTRAN) type accident could also result in fuel rod failure and subsequent release of fission products similar to the LOC type accident. The NRC Regulatory Guides 1.3 and 1.4, for LOC type accidents, state that "Twenty five percent of the equilibrium radioactive iodine inventory developed from maximum full power operation of the core should be assumed to be immediately available for leakage from the primary reactor containment", and that "One hundred percent of the equilibrium radioactive noble gas inventory ... be immediately available for leakage...". This assumption necessarily implies that like fractions of the iodine and noble gases be in the fuel-cladding gap available for release. These release fractions have been estimated¹ to be about 100 times too large.

The NRC Regulatory Guide 1.25 states that for a fuel handling accident "All of the gap activity in the damaged rods is released and consists of 10% of the total noble gases other than ^{85}Kr , 30% of the ^{85}Kr , and 10% of the total radioactive iodine in the rods at the time of the accident." These assumptions also imply that the release fractions during operation were of similar magnitude, that is, 10 to 30%.

The American Nuclear Society proposed standard ANSI/ANS 5.4 for calculating the release of fission products is to be used with the GAPCON-2 fuel behavior code for revision of the NRC regulatory guides.¹ Based on the comparison of the IFA-430 data with the ANS 5.4 calculations, it appears that the ANS model does a reasonable job of predicting the steady state release fraction for xenon and iodine and somewhat underpredicts the krypton release fraction. Comparison of the measured and ANS 5.4 calculated release fractions with the regulatory guide assumptions points out the overconservatism of the regulatory guides. The measured and calculated release fractions for xenon, krypton, and iodine were all in the range 10^{-6} to 10^{-3} , at least two orders of magnitude less than that assumed in a fuel handling accident and three orders of magnitude less than that assumed for a successfully terminated LOC type accident in which fuel peak temperature is less than ~ 1450 K.

Thus, it appears that the data from the IFA-430 experiment support both the use of the ANS 5.4 proposed standard to estimate noble gas and iodine release for steady state conditions and support the NRC estimates of the over-conservatisms of the assumptions for fission product release in the NRC Regulatory Guides 1.25, 1.3, and 1.4. However, the ANS 5.4 model apparently needs further development to account for precursor effects on Kr release and to better predict the very short lived isotopes of Xe.

The conclusions drawn from the fission product release tests and comparison of the results with release models are:

1. The release rates of xenon and krypton fission gas isotopes can be measured during nuclear operation with reasonable accuracy. The measurements are repeatable and consistent.
2. The gap inventory (at power) of ^{131}I and ^{135}I can be determined by measuring the daughter products following reactor shutdown. The results show that the iodine release is of the same order of magnitude as xenon release.
3. The measured relationship between the R/B ratio and λ indicates that the release can be described in terms of diffusion even for low (~ 850 K bulk average) fuel temperatures.

4. The ANS 5.4 fission product release model calculations for ^{135}Xe and ^{133}Xe are within the uncertainty bands of the IFA-430 data; however, for the shorter lived (< 15 minute) Xe isotopes the calculated release is less than the measured by a factor of ~ 2 .
5. The ANS 5.4 calculated Kr release fractions are less than the measured data by factors of 2 to 4 for ^{89}Kr , ^{88}Kr , ^{87}Kr , and $^{85\text{m}}\text{Kr}$.
6. The ANS 5.4 calculated release fractions for ^{131}I is within the uncertainty band of the data and the calculated ^{135}I release fraction is higher than the data by a factor of ~ 2 .
7. The diffusion release model of Friskney and Turnbull, which takes into account the effect of precursors, calculates R/B ratios which show good agreement with the data when the pellet true surface area includes the effects of pellet cracking. More significantly, the model predicts the detailed relationship between the different isotopes, indicating that the model probably includes the correct mechanisms accounting for precursor effects and element-dependent diffusion coefficients.

The experiments to date have measured only the shorter lived (less than a few weeks) xenons, kryptons, and iodines. The system is being modified to obtain data on longer lived isotopes such as ^{85}Kr (10 year half-life) which should behave much the same as the stable fission gases. In addition, the release during power ramps and at higher temperatures will be measured during future tests.

7. REFERENCES

1. R. O. Meyer, Current Fuels Licensing Issues, February 1979, Seminar for Korea Atomic Energy Research Institute, Nuclear Regulatory Commission Reactor Fuels Section.
2. Nuclear Regulatory Commission, The Role of Fission Gas in Reactor Licensing NUREG-75/007 November 1975.
3. Proposed ANS-WG 5.4 Standard, Method for Calculating the Release of Fission Products from Oxide Fuel, American Nuclear Society, November 1979, Rev. 1, May 1980.
4. U. N. Rausch, F. E. Panisko, "ANS5.4: A Computer Subroutine for Predicting Fission Gas Release," NUREG/CR1213 PNL-3077, August 1979.
5. United States Nuclear Regulatory Commission, Division of Reactor Safety Research, Water Reactor Safety Research Program, A Description of Current and Planned Research, NUREG-0006, February 1979.
6. R. M. Carroll and O. Sisman, "In-Pile Fission Gas Release From Single Crystal UO_2 ," Nuc Sci & Eng 21, 1965, pp. 147-158.
7. R. M. Carroll, et al., "Fission Density, Burnup, and Temperature Effects on Fission-Gas Release from UO_2 ," Nuc Sci & Eng 38, 1969, pp. 143-155.
8. G. A. Friskney and J. A. Turnbull, "The Characteristics of Fission Gas Release From UO_2 During Irradiation," Jrnl Nuc Mtrl, Vol. 79, No. 1, January 1979.
9. J. A. Turnbull, et al., "The Release of Radioactive Gases From UO_2 During Irradiation," Jrnl Nuc Mtrl, Vol. 67, No. 3, August 1977.

10. G. J. Greatley, R. HarGreaves, "The Measured Emission of Fission Product Gases From Operating UO_2 Fuel," Jrnl Nuc Mtrl, Vol. 79, 1979, pp. 235-245.
11. A. D. Appelhans, et al., Cracking and Relocation of UO_2 Fuel During Initial Nuclear Operation, NUREG/CR-1425 EGG-2032, May 1980.
12. A. D. Appelhans, S. J. Dagdjartsson, IFA-430 Fission Product Measurement System Description and Scoping Test Results, EGG-TFBP-5026, December, 1979.
13. M. J. Bell, ORIGEN - The ORNL Isotope Generation and Depletion Code, ORNL-4628, 1973.
14. D. R. Olander, "Fundamental Aspects of Nuclear Reactor Fuel Elements," TID-26711-P1, 1976.
15. G. A. Berna, et al., FRAPCON-2: A Computer Code for the Steady-State Analysis of Oxide Fuel Rods, to be published, Reference FRAPCON-1 CDAP-TR-78-032, August 1978.
16. J. A. Turnbull and G. A. Friskney, to be published.
17. C. A. Friskney and M. V. Speight, A Calculation on the In-Pile Diffusional Release of Fission Products Forming a General Decay Chain, JRNL NUC MTRL Vol 62, 1976, pp. 89-94.
18. J. Williams, The Postirradiation Examination of Three Fuel Rods From the IFA-429 Experiment Irradiated in the Halder Reactor, AERE-R 9619, November 1979.

APPENDIX A
RELEASE RATE CALCULATIONS

This appendix provides details of the calculation of the release rates for the Noble gases and iodine from the gamma spectrometer data.

Noble Gas Release Rate Equations

The fission gases swept out of the fuel rod flow by the gamma spectrometer which measures the average concentration of the fission gases in the gas stream. The concentration is determined using

$$C_D = \frac{A}{T_\ell \epsilon B V_p \left(\frac{T}{T_p}\right) \left(\frac{P}{P}\right) \lambda} \quad (A-1)$$

where C_D = concentration at the detector location (atoms/cc)

A = area of gamma peak for isotope of interest

T_ℓ = live time of spectra

ϵ = detector absolute efficiency

B = gamma ray abundance

V_p = volume of sample viewed by detector

T = standard temperature (273 K)

T_p = temperature of gas sample

P = standard pressure (0.1013 MPa)

λ = decay constant for isotope of interest

The specific activity, A_D , is given by

$$A_D = \lambda C_D \quad (A-2)$$

and the specific activity of the gas at the detector is related to the specific activity of the gas in the fuel rod, A_R , by

$$A_D = e^{-\lambda t_d} A_R \quad (A-3)$$

where t_d is the delay time for transit of the gas from the fuel rod to the detector.

Equation (A-3) implies that

$$\lambda C_D = \lambda e^{-\lambda t_d} C_R \quad (A-4)$$

where C_R is the concentration at the fuel rod. The free volume of the fuel rod at standard temperature and pressure (STP) is

$$V_R(\text{STP}) = V_R \frac{T_0}{T_R} \frac{P_R}{P_0} \quad (A-5)$$

where the subscript R refers to conditions at the fuel rod. The concentration of an isotope in the gas in the fuel rod is also given by

$$C_R = \frac{Rt}{V_R(\text{STP})} \quad (A-6)$$

where R is the isotopic release rate and t is the time that the volume of gas is in the fuel rod. Combining equations (A-5) and (A-6)

$$C_R = \frac{Rt}{V_R} \frac{T_R}{T_0} \frac{P_0}{P_R} \quad (A-7)$$

and noting that the time the gas is in the fuel rod is given by

$$t = \frac{V_R(\text{STP})}{f(\text{STP})} \quad (\text{A-8})$$

where f is the flow rate of the gas, equation (A-7) can be reduced to

$$C_R = \frac{R}{f(\text{STP})} \quad (\text{A-9})$$

Thus, the release rate can be determined, combining Equations (A-9), (A-4), and (A-1),

$$R = \frac{f A e^{-\lambda t} d_T p_0}{T_e \epsilon B V_p T_o p \lambda} \quad (\text{A-10})$$

Iodine Release Rate Equations

The iodine being released from the fuel rod plates out on the fuel and cladding and subsequently decays to xenon. Thus, the amount of iodine that has plated out, i.e. the gap inventory, can be determined by shutting down the reactor, which effectively stops diffusion of Xe from the fuel, and measuring the Xe coming from the iodine decay.

At the time of reactor shutdown there are $N_i(0)$ iodine atoms (of isotope i) plated out in the fuel rod at time $t = 0$. The $N_i(0)$ iodine atoms are decaying to Xe and thus are released at a rate, R_x ,

$$R_x = S \lambda_i N_i \quad (\text{A-11})$$

where S is the branching ratio. At $t > 0$ the release rate is

$$R_x(t) = S \lambda_i N_i(0) e^{-\lambda_i t} \quad (\text{A-12})$$

which, if $R_x(t)$ is measured, allows the iodine inventory at $t = 0$, $N_i(0)$, to be determined,

$$N_i(0) = \frac{R_{Xe} \lambda_i t}{S \lambda_i} \quad (A-13)$$

Equation (A-13) is applied to determine the ^{135}I and ^{133}I inventory following a reactor scram and, if the release rate of the iodine was at equilibrium, i.e. the amount being released was equal to the amount decaying per unit time, then the iodine release rate is

$$R_i(0) = \lambda_i N_i(0) \quad (A-14)$$

The equilibrium condition is confirmed by monitoring the ^{135}Xe and ^{133}Xe release rate at power prior to the reactor shutdown. The measured release rate of Xe at power is combined of Xe being released as Xe from the fuel and Xe being released as a result of iodine decay. Thus, when the Xe release rate at power is constant in time, both the iodine release and Xe release from the fuel are at equilibrium and Equation (A-14) can be used to determine the equilibrium release rate. This approach was used to determine the ^{135}I and ^{133}I release rates.

To determine the ^{131}I gap inventory the fuel rod is kept closed following reactor shutdown for a time t_s (typically 2-3 days) during which most of the ^{133}I decays to ^{133}Xe , and a small part of the ^{131}I decays to ^{131}Xe . The rod is then flushed to remove the ^{133}Xe , which interferes with measurement of the ^{131}Xe , and once again closed. The ^{131}I continues to decay to ^{131}Xe and, at a time t_u the ^{131}Xe content reaches a maximum, at which time it is flushed from the rod and measured. The measured ^{131}Xe inventory at t_u can then be related to the ^{131}I inventory and thus to $N_i(0)$, the ^{131}I gap inventory at shutdown. The following is a derivation of the equations used to determine the iodine gap inventory from the measured xenon concentration.

The xenon rate equation for times after shutdown is

$$\frac{dN_x}{dt} = \lambda_i N_i - \lambda_x N_x \quad (\text{A-15})$$

and for an initial concentration of iodine, $N_i(0)$, and xenon, $N_x(0)$, the Xe concentration as a function time is

$$N_x(t) = N_x e^{-\lambda_x t} + \frac{\lambda_i N_i(0)}{\lambda_i - \lambda_x} (e^{-\lambda_x t} - e^{-\lambda_i t}) \quad (\text{A-16})$$

However, the rod is flushed at t_s , thus $N_x(0)$ is zero at t_s , and at $t = t_u$

$$N_x(t_u) = \frac{\lambda_i N_i(t_s)}{\lambda_i - \lambda_x} [e^{-\lambda_x(t_u - t_s)} - e^{-\lambda_i(t_u - t_s)}] \quad (\text{A-17})$$

which, substituting $N_i(t_s) = N_i(0)e^{-\lambda_i t_s}$ reduces to

$$N_x(t_u) = \frac{\lambda_i N_i(0) e^{-\lambda_x t_u}}{\lambda_i + \lambda_x} [e^{(\lambda_x - \lambda_i)t_u} - e^{(\lambda_x - \lambda_i)t_s}] \quad (\text{A-18})$$

The ^{131}I decay to xenon includes branches to ^{131m}Xe and ^{131}Xe ; thus, when measuring ^{131m}Xe equation (A-18) has to include the branching ratio, S ,

$$N_x(t_u) = \frac{S \lambda_i N_i(0) e^{-\lambda_x t_u}}{\lambda_i + \lambda_x} [e^{(\lambda_x - \lambda_i)t_u} - e^{(\lambda_x - \lambda_i)t_s}] \quad (\text{A-19})$$

If the xenon in the rod at $t = t_u$, $N_x(t_u)$, is flushed out and swept by the detector at a constant flow rate, the total number of disintegrations that occur in the sample volume viewed by the detector can be shown to be

$$\lambda_x N_x t_2 = \frac{\lambda_x N_x P_2 V_2}{f_0 P_0} \quad (\text{A-20})$$

where f_0 is the flow rate at STP and t_2 is the transit time of the gas by the detector. The total number of disintegrations counted by the detector (peak area) is

$$A = \frac{\epsilon B \lambda_x P_2 V_2 N_x}{f_0 P_0} \quad (\text{A-21})$$

which, when combined with Equation (A-19), permits the gap inventory at $t = 0$ (shutdown) to be determined from the measurement of A and associated parameters,

$$N_i(0) = \frac{[\lambda_x - \lambda_i] e^{\lambda_x t_u}}{S \lambda_i} \frac{f_0 P_0 A}{\epsilon B \lambda_x P_2 V_2} \left[e^{(\lambda_x - \lambda_i) t_u} - e^{(\lambda_x - \lambda_i) t_s} \right]^{-1} \quad (\text{A-22})$$

FRACTIONAL RELEASE CALCULATION

The gap inventory just prior to shutdown was determined using Equation (A-22) and the measured values for the variables. The total rod inventory was determined by simplifying the rod operating history for the period prior to shutdown and calculating the total inventory. Figure A-1 shows the actual rod power history (solid line) and the simplified history used in the calculations. Tables A-1 and A-2 list the values used to calculate the total non-decayed inventory at shutdown.

The measured gap inventory divided by the calculated total rod inventory gives the release fraction. The measured gap inventories were 7.87×10^{15} atoms for ^{133}I and 3.39×10^{15} atoms for ^{131}I . Thus the release fractions are

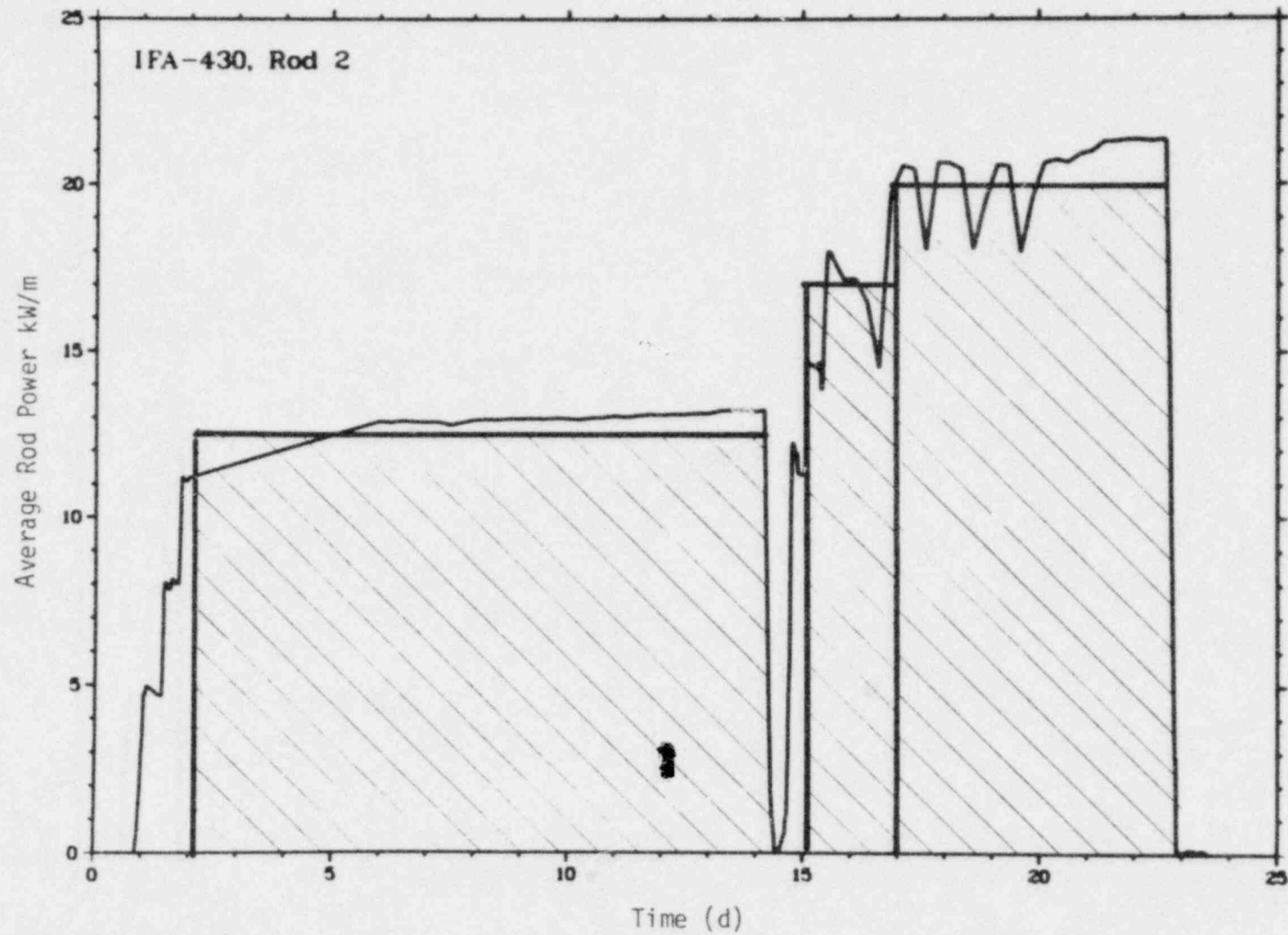


Figure A-1. Rod 2 average power from March 28 through April 18, 1980 and simplified power history (dashed region) used to calculate total rod iodine inventories.

$$F(^{131}\text{I}) = 2.3 \times 10^{-4}$$

and

$$F(^{133}\text{I}) = 1.5 \times 10^{-3}.$$

The FRAPCON-2 code with the ANS 5.4 fission gas release model was also used to calculate the fractional release. The rod simplified rod power history shown in Figure A-1 was run in FRAPCON-2 and the fractional release during each power-time period calculated with ANS 5.4. The fractional release was then multiplied by the inventory remaining from each time-power period at shutdown and divided by the total inventory present at shutdown to get the integrated release fraction at shutdown.

TABLE A-1 ROD 2 ^{131}I INVENTORY CALCULATION
INPUT AND RESULTS

| Rod Power (kW) | Fission Rate (s^{-1}) | Irradiation Time (s) | Inventory at Shutdown (atoms) |
|-------------------|--|----------------------------|-------------------------------------|
| 15.6 | 5.01×10^{14} | 1.04×10^6 | 4.24×10^{18} |
| 19.8 | 6.36×10^{14} | 1.30×10^5 | 1.26×10^{18} |
| 24.0 | 7.71×10^{14} | 5.62×10^5 | 9.42×10^{18} |
| | | TOTAL | 1.5×10^{19} atoms |

TABLE A-2 ROD 2 ^{133}I INVENTORY CALCULATION
INPUT AND RESULTS

| Rod Power (kW) | Fission Rate (s^{-1}) | Irradiation Time (s) | Inventory at Shutdown |
|-------------------|--|----------------------------|--------------------------|
| 15.6 | 5.01×10^{14} | 1.04×10^6 | 2.6×10^{15} |
| 19.8 | 6.36×10^{14} | 1.30×10^5 | 1.7×10^{16} |
| 24.0 | 7.71×10^{14} | 5.62×10^5 | 5.4×10^{18} |
| | | TOTAL | 5.4×10^{18} |

APPENDIX B
SUMMARY OF ORIGEN CALCULATIONS

W. Olson

Instrumented Fuel Assembly 430 (IFA-430) is being used to measure the amounts of the various fission product gases and volatiles released to the fuel-cladding gap during reactor operation.

This appendix provides calculated inventories and production rates for fission product gases in these fuel rods. These inventories are used, together with the experimentally measured amounts of the gases swept out of the rods, to determine the release-to-birth (R/B) ratios (fractional release).

The calculations were based on a neutron energy spectrum for the IFA-430 test fuel obtained using the RAFFLE¹ Monte Carlo code. This neutron spectrum was used to determine average cross sections and to produce a 3-group spectrum for use in the ORIGEN² isotope depletion and buildup code which calculates the fission product inventories.

Inventory errors were estimated for the gaseous fission product isotopes of interest. Uncertainties arising from the spectrum calculation are estimated to be less than 1%. Uncertainties arising from the yield data are up to 4% (1 σ confidence level) and equal the uncertainties in the ENDF data. A uniform power has been assumed for a period of 60 hours preceding the fission gas measurement tests. The fractional uncertainty in the measurement of the power transfers directly to the fission product inventories, and is estimated to be the most significant factor in the uncertainty of the calculations.

Table B-1 gives selected results of the ORIGEN code for a rod power of 26 kW; Table B-2 provides a typical ORIGEN printout; and Table B-3 is an example of the ORIGEN input deck with a 26 kW rod power in the final irradiation period.

CONCLUSIONS AND SUGGESTIONS

1. Approximations used in the spectrum calculations are not a major source of error due to the preponderance of fission in U-235. The errors in fission product inventories from this source are under one percent.
2. Fission product yield data cause uncertainties in the fission product inventories of up to 4% at the 1σ confidence level.
3. Inventories for the isotopes of interest are quite insensitive to the power history except during the last few days before the inventories are desired. This insensitivity is due to the short half-lives involved and would not be true for long half-life fission products. The insensitivity also reflects that most of the fission occurs in U-235 throughout in the burnup range considered. A change in the integrated power (before the final burn) of 10% showed negligible effects on the isotopes of interest because of this preponderance of U-235 fission.
4. Errors in the power estimates in the time period immediately before the inventories are calculated are very important. If this history is an exposure at constant power, the fractional error in the inventory is equal to the fractional error in the power estimate.
5. Uncertainties in the energy-per-fission value are transmitted to the fission product inventories. A value of 200 MeV/fission has been assumed in the calculations. If a value of 195 MeV/fission should have been used, then the inventories of the report should be corrected by multiplying by 200/195.
6. Calculations have been made on the basis of an average IFA-430 fuel rod. The fuel mass of this average rod differs about 1.2 percent from that of each individual rod. This will have no noticeable effect on the calculated inventories.

7. The inventory data given in this Appendix for nuclides other than volatile fission gases should also be quite accurate (generally less than 1% error from spectrum effects) for the power history used. There will be larger errors for decay chains with a higher absorption nuclide (such as Sm-149, for example) since their absorption cross sections haven't been updated to the IFA-430 spectrum. We also note that for longer half-life materials (more than 12 hours or so) or those preceded in the decay chain by longer half-life materials, and equilibrium between production and decay will not have been established.

8. The inventories of interest may be adjusted in direct proportion to the power during the final 66-hour exposure, with the exception of the Xe-135 inventory. This proportionality was tested between 26 and 38 kW/rod, yielding inventories for the krypton and xenon isotopes of interest which were directly proportional to power. For the Xe-135 inventory, comparison of the 26 and 38 kW/rod ORIGEN calculations showed that the Xe-135 inventory changes at half the fractional rate that power changes.

Summarizing, the inventories of interest and the Xe-135 production rate for a constant (for 66 hours) power of, 26 kW/rod are given in Table B-1. To obtain the inventories and production rates (except the Xe-135 inventory) at a power of for example, 28.1 kW/rod, multiply the tabulated values by 28.1/26. To obtain the Xe-135 inventory at 28.1 kW/rod, multiply the 26 kW/rod value by 27.05/26. For power values appreciably outside the range examined, ORIGEN should be rerun if the Xe-135 inventory is needed. Also, for any case where a nonconstant power is used for the final 66-hour irradiation, a new ORIGEN calculation is necessary.

TABLE B-1 GASEOUS FISSION PRODUCT INVENTORY PER PIN
(following 66 hours exposure at 26 kW)

| <u>Isotope</u> | <u>Inventory (curies) ENDF/B Version 4 Yield Data</u> | <u>Inventory (curies) ENDF/B Version 5 Yield Data</u> |
|----------------|---|---|
| Kr 85m | 280 | 280 |
| Kr 87 | 545 | 539 |
| Kr 88 | 771 | 763 |
| Kr 89 | 1000 | 983 |
| Xe 135* | 805 | 789 |
| Xe 137 | 1350 | 1330 |
| Xe 138 | 1360 | 1400 |
| Xe 139 | 1120 | 1120 |

* The 66 hour production rate of Xe-135, converted to curies for ease of comparison (although not a proper unit) is 1480 curies (V4) and 1470 curies (V5). That is, 1470 curies of Xe-135 undergo radioactive decay at a rate equal to the production rate of Xe-135.

POOR ORIGINAL

TABLE B-2. SELECTED ORIGIN CALCULATIONS FOR 26 KW ROD POWER

HALDEN-IFA-430 PIN-SHUTDOWN AND FINAL BURN
 POWER = 234W, 30KRUUF = 5.5MW, FLUX = 1.15E+13N/CM*2-SEC
 BASIS = FALDEN430 PIN-1110G U-97, 856-U-235

| | INITIAL | 609-HR. | 624-HR. | 630-HR. | 636-HR. | 642-HR. | 648-HR. | 654-HR. | 660-HR. | 666-HR. |
|-----|----------|----------|----------|----------|----------|----------|----------|----------|----------|----------|
| 80 | 1.97E+01 | 1.97E+01 | 1.97E+01 | 1.97E+01 | 1.97E+01 | 1.97E+01 | 1.97E+01 | 1.97E+01 | 1.97E+01 | 1.97E+01 |
| 81 | 1.38E+00 | 1.38E+00 | 1.38E+00 | 1.38E+00 | 1.38E+00 | 1.38E+00 | 1.38E+00 | 1.38E+00 | 1.38E+00 | 1.38E+00 |
| 82 | 1.14E+00 | 1.14E+00 | 1.14E+00 | 1.14E+00 | 1.14E+00 | 1.14E+00 | 1.14E+00 | 1.14E+00 | 1.14E+00 | 1.14E+00 |
| 83 | 0.46E+04 | 0.46E+04 | 0.46E+04 | 0.46E+04 | 0.46E+04 | 0.46E+04 | 0.46E+04 | 0.46E+04 | 0.46E+04 | 0.46E+04 |
| 84 | 0.66E+04 | 0.66E+04 | 0.66E+04 | 0.66E+04 | 0.66E+04 | 0.66E+04 | 0.66E+04 | 0.66E+04 | 0.66E+04 | 0.66E+04 |
| 85 | 0.25E+04 | 0.25E+04 | 0.25E+04 | 0.25E+04 | 0.25E+04 | 0.25E+04 | 0.25E+04 | 0.25E+04 | 0.25E+04 | 0.25E+04 |
| 86 | 0.98E+01 | 0.98E+01 | 0.98E+01 | 0.98E+01 | 0.98E+01 | 0.98E+01 | 0.98E+01 | 0.98E+01 | 0.98E+01 | 0.98E+01 |
| 87 | 0.57E+01 | 0.57E+01 | 0.57E+01 | 0.57E+01 | 0.57E+01 | 0.57E+01 | 0.57E+01 | 0.57E+01 | 0.57E+01 | 0.57E+01 |
| 88 | 0.57E+02 | 0.57E+02 | 0.57E+02 | 0.57E+02 | 0.57E+02 | 0.57E+02 | 0.57E+02 | 0.57E+02 | 0.57E+02 | 0.57E+02 |
| 89 | 0.22E+02 | 0.22E+02 | 0.22E+02 | 0.22E+02 | 0.22E+02 | 0.22E+02 | 0.22E+02 | 0.22E+02 | 0.22E+02 | 0.22E+02 |
| 90 | 0.37E+02 | 0.37E+02 | 0.37E+02 | 0.37E+02 | 0.37E+02 | 0.37E+02 | 0.37E+02 | 0.37E+02 | 0.37E+02 | 0.37E+02 |
| 91 | 0.09E+02 | 0.09E+02 | 0.09E+02 | 0.09E+02 | 0.09E+02 | 0.09E+02 | 0.09E+02 | 0.09E+02 | 0.09E+02 | 0.09E+02 |
| 92 | 0.09E+02 | 0.09E+02 | 0.09E+02 | 0.09E+02 | 0.09E+02 | 0.09E+02 | 0.09E+02 | 0.09E+02 | 0.09E+02 | 0.09E+02 |
| 93 | 0.09E+02 | 0.09E+02 | 0.09E+02 | 0.09E+02 | 0.09E+02 | 0.09E+02 | 0.09E+02 | 0.09E+02 | 0.09E+02 | 0.09E+02 |
| 94 | 0.09E+02 | 0.09E+02 | 0.09E+02 | 0.09E+02 | 0.09E+02 | 0.09E+02 | 0.09E+02 | 0.09E+02 | 0.09E+02 | 0.09E+02 |
| 95 | 0.09E+02 | 0.09E+02 | 0.09E+02 | 0.09E+02 | 0.09E+02 | 0.09E+02 | 0.09E+02 | 0.09E+02 | 0.09E+02 | 0.09E+02 |
| 96 | 0.09E+02 | 0.09E+02 | 0.09E+02 | 0.09E+02 | 0.09E+02 | 0.09E+02 | 0.09E+02 | 0.09E+02 | 0.09E+02 | 0.09E+02 |
| 97 | 0.09E+02 | 0.09E+02 | 0.09E+02 | 0.09E+02 | 0.09E+02 | 0.09E+02 | 0.09E+02 | 0.09E+02 | 0.09E+02 | 0.09E+02 |
| 98 | 0.09E+02 | 0.09E+02 | 0.09E+02 | 0.09E+02 | 0.09E+02 | 0.09E+02 | 0.09E+02 | 0.09E+02 | 0.09E+02 | 0.09E+02 |
| 99 | 0.09E+02 | 0.09E+02 | 0.09E+02 | 0.09E+02 | 0.09E+02 | 0.09E+02 | 0.09E+02 | 0.09E+02 | 0.09E+02 | 0.09E+02 |
| 100 | 0.09E+02 | 0.09E+02 | 0.09E+02 | 0.09E+02 | 0.09E+02 | 0.09E+02 | 0.09E+02 | 0.09E+02 | 0.09E+02 | 0.09E+02 |

POOR ORIGINAL

TABLE B-2. SELECTED ORIGIN CALCULATIONS
FOR 26 KW ROD POWER (cont'd)

HALDEN-IT-A-530 P4-SHUTDOWN AND FINAL BURN
POWER= 30KW, TURNUP= 5.1%
NUCLIE RADIACTIVITY, CURIES
BASIS = HALDEN43J PIN-1110G U-97.85G-U-235

| | MYIAL | 800.HR. | 624.HR. | 630.HR. | 642.HR. | 648.HR. | 654.HR. | 660.HR. | 666.HR. |
|------|----------|----------|----------|----------|----------|----------|----------|----------|----------|
| 120M | 1.27E+01 | 1.27E+01 | 1.27E+01 | 1.27E+01 | 1.27E+01 | 1.27E+01 | 1.27E+01 | 1.27E+01 | 1.27E+01 |
| 125M | 1.27E+01 | 1.27E+01 | 1.27E+01 | 1.27E+01 | 1.27E+01 | 1.27E+01 | 1.27E+01 | 1.27E+01 | 1.27E+01 |
| 130M | 1.27E+01 | 1.27E+01 | 1.27E+01 | 1.27E+01 | 1.27E+01 | 1.27E+01 | 1.27E+01 | 1.27E+01 | 1.27E+01 |
| 135M | 1.27E+01 | 1.27E+01 | 1.27E+01 | 1.27E+01 | 1.27E+01 | 1.27E+01 | 1.27E+01 | 1.27E+01 | 1.27E+01 |
| 140M | 1.27E+01 | 1.27E+01 | 1.27E+01 | 1.27E+01 | 1.27E+01 | 1.27E+01 | 1.27E+01 | 1.27E+01 | 1.27E+01 |
| 145M | 1.27E+01 | 1.27E+01 | 1.27E+01 | 1.27E+01 | 1.27E+01 | 1.27E+01 | 1.27E+01 | 1.27E+01 | 1.27E+01 |
| 150M | 1.27E+01 | 1.27E+01 | 1.27E+01 | 1.27E+01 | 1.27E+01 | 1.27E+01 | 1.27E+01 | 1.27E+01 | 1.27E+01 |
| 155M | 1.27E+01 | 1.27E+01 | 1.27E+01 | 1.27E+01 | 1.27E+01 | 1.27E+01 | 1.27E+01 | 1.27E+01 | 1.27E+01 |
| 160M | 1.27E+01 | 1.27E+01 | 1.27E+01 | 1.27E+01 | 1.27E+01 | 1.27E+01 | 1.27E+01 | 1.27E+01 | 1.27E+01 |
| 165M | 1.27E+01 | 1.27E+01 | 1.27E+01 | 1.27E+01 | 1.27E+01 | 1.27E+01 | 1.27E+01 | 1.27E+01 | 1.27E+01 |
| 170M | 1.27E+01 | 1.27E+01 | 1.27E+01 | 1.27E+01 | 1.27E+01 | 1.27E+01 | 1.27E+01 | 1.27E+01 | 1.27E+01 |
| 175M | 1.27E+01 | 1.27E+01 | 1.27E+01 | 1.27E+01 | 1.27E+01 | 1.27E+01 | 1.27E+01 | 1.27E+01 | 1.27E+01 |
| 180M | 1.27E+01 | 1.27E+01 | 1.27E+01 | 1.27E+01 | 1.27E+01 | 1.27E+01 | 1.27E+01 | 1.27E+01 | 1.27E+01 |
| 185M | 1.27E+01 | 1.27E+01 | 1.27E+01 | 1.27E+01 | 1.27E+01 | 1.27E+01 | 1.27E+01 | 1.27E+01 | 1.27E+01 |
| 190M | 1.27E+01 | 1.27E+01 | 1.27E+01 | 1.27E+01 | 1.27E+01 | 1.27E+01 | 1.27E+01 | 1.27E+01 | 1.27E+01 |
| 195M | 1.27E+01 | 1.27E+01 | 1.27E+01 | 1.27E+01 | 1.27E+01 | 1.27E+01 | 1.27E+01 | 1.27E+01 | 1.27E+01 |
| 200M | 1.27E+01 | 1.27E+01 | 1.27E+01 | 1.27E+01 | 1.27E+01 | 1.27E+01 | 1.27E+01 | 1.27E+01 | 1.27E+01 |
| 205M | 1.27E+01 | 1.27E+01 | 1.27E+01 | 1.27E+01 | 1.27E+01 | 1.27E+01 | 1.27E+01 | 1.27E+01 | 1.27E+01 |
| 210M | 1.27E+01 | 1.27E+01 | 1.27E+01 | 1.27E+01 | 1.27E+01 | 1.27E+01 | 1.27E+01 | 1.27E+01 | 1.27E+01 |
| 215M | 1.27E+01 | 1.27E+01 | 1.27E+01 | 1.27E+01 | 1.27E+01 | 1.27E+01 | 1.27E+01 | 1.27E+01 | 1.27E+01 |
| 220M | 1.27E+01 | 1.27E+01 | 1.27E+01 | 1.27E+01 | 1.27E+01 | 1.27E+01 | 1.27E+01 | 1.27E+01 | 1.27E+01 |
| 225M | 1.27E+01 | 1.27E+01 | 1.27E+01 | 1.27E+01 | 1.27E+01 | 1.27E+01 | 1.27E+01 | 1.27E+01 | 1.27E+01 |
| 230M | 1.27E+01 | 1.27E+01 | 1.27E+01 | 1.27E+01 | 1.27E+01 | 1.27E+01 | 1.27E+01 | 1.27E+01 | 1.27E+01 |
| 235M | 1.27E+01 | 1.27E+01 | 1.27E+01 | 1.27E+01 | 1.27E+01 | 1.27E+01 | 1.27E+01 | 1.27E+01 | 1.27E+01 |
| 240M | 1.27E+01 | 1.27E+01 | 1.27E+01 | 1.27E+01 | 1.27E+01 | 1.27E+01 | 1.27E+01 | 1.27E+01 | 1.27E+01 |
| 245M | 1.27E+01 | 1.27E+01 | 1.27E+01 | 1.27E+01 | 1.27E+01 | 1.27E+01 | 1.27E+01 | 1.27E+01 | 1.27E+01 |
| 250M | 1.27E+01 | 1.27E+01 | 1.27E+01 | 1.27E+01 | 1.27E+01 | 1.27E+01 | 1.27E+01 | 1.27E+01 | 1.27E+01 |
| 255M | 1.27E+01 | 1.27E+01 | 1.27E+01 | 1.27E+01 | 1.27E+01 | 1.27E+01 | 1.27E+01 | 1.27E+01 | 1.27E+01 |
| 260M | 1.27E+01 | 1.27E+01 | 1.27E+01 | 1.27E+01 | 1.27E+01 | 1.27E+01 | 1.27E+01 | 1.27E+01 | 1.27E+01 |

POOR ORIGINAL

TABLE B-2. SELECTED ORIGIN CALCULATIONS FOR 26 kW ROD POWER (cont'd)

HALDEN-31A-30 PIN-SHUTDOWN AND FINAL BURN
POWER = 0.3MW, BURNUP = 5. MW, FLUX = 1.15E+13n/cm²+2-SEC

NUCLIDE RADIOACTIVITY, CURIES
JALIS - HALDEN 30 PIN-11106 U-97.85G-U-235

| ISOTOPE | 600.HR. | 624.HR. | 630.HR. | 636.HR. | 642.HR. | 648.HR. | 654.HR. | 660.HR. | 666.HR. |
|---------|----------|----------|----------|----------|----------|----------|----------|----------|----------|
| 238U | 1.13E+01 | 1.13E+01 | 1.13E+01 | 1.13E+01 | 1.13E+01 | 1.13E+01 | 1.13E+01 | 1.13E+01 | 1.13E+01 |
| 235U | 1.13E+02 | 1.13E+02 | 1.13E+02 | 1.13E+02 | 1.13E+02 | 1.13E+02 | 1.13E+02 | 1.13E+02 | 1.13E+02 |
| 239Pu | 1.13E+03 | 1.13E+03 | 1.13E+03 | 1.13E+03 | 1.13E+03 | 1.13E+03 | 1.13E+03 | 1.13E+03 | 1.13E+03 |
| 240Pu | 1.13E+04 | 1.13E+04 | 1.13E+04 | 1.13E+04 | 1.13E+04 | 1.13E+04 | 1.13E+04 | 1.13E+04 | 1.13E+04 |
| 241Pu | 1.13E+05 | 1.13E+05 | 1.13E+05 | 1.13E+05 | 1.13E+05 | 1.13E+05 | 1.13E+05 | 1.13E+05 | 1.13E+05 |
| 242Pu | 1.13E+06 | 1.13E+06 | 1.13E+06 | 1.13E+06 | 1.13E+06 | 1.13E+06 | 1.13E+06 | 1.13E+06 | 1.13E+06 |
| 243Am | 1.13E+07 | 1.13E+07 | 1.13E+07 | 1.13E+07 | 1.13E+07 | 1.13E+07 | 1.13E+07 | 1.13E+07 | 1.13E+07 |
| 244Cm | 1.13E+08 | 1.13E+08 | 1.13E+08 | 1.13E+08 | 1.13E+08 | 1.13E+08 | 1.13E+08 | 1.13E+08 | 1.13E+08 |
| 245Cm | 1.13E+09 | 1.13E+09 | 1.13E+09 | 1.13E+09 | 1.13E+09 | 1.13E+09 | 1.13E+09 | 1.13E+09 | 1.13E+09 |
| 246Cm | 1.13E+10 | 1.13E+10 | 1.13E+10 | 1.13E+10 | 1.13E+10 | 1.13E+10 | 1.13E+10 | 1.13E+10 | 1.13E+10 |
| 247Cm | 1.13E+11 | 1.13E+11 | 1.13E+11 | 1.13E+11 | 1.13E+11 | 1.13E+11 | 1.13E+11 | 1.13E+11 | 1.13E+11 |
| 248Cm | 1.13E+12 | 1.13E+12 | 1.13E+12 | 1.13E+12 | 1.13E+12 | 1.13E+12 | 1.13E+12 | 1.13E+12 | 1.13E+12 |
| 249Bk | 1.13E+13 | 1.13E+13 | 1.13E+13 | 1.13E+13 | 1.13E+13 | 1.13E+13 | 1.13E+13 | 1.13E+13 | 1.13E+13 |
| 250Cf | 1.13E+14 | 1.13E+14 | 1.13E+14 | 1.13E+14 | 1.13E+14 | 1.13E+14 | 1.13E+14 | 1.13E+14 | 1.13E+14 |
| 251Cf | 1.13E+15 | 1.13E+15 | 1.13E+15 | 1.13E+15 | 1.13E+15 | 1.13E+15 | 1.13E+15 | 1.13E+15 | 1.13E+15 |
| 252Cf | 1.13E+16 | 1.13E+16 | 1.13E+16 | 1.13E+16 | 1.13E+16 | 1.13E+16 | 1.13E+16 | 1.13E+16 | 1.13E+16 |
| 253Cf | 1.13E+17 | 1.13E+17 | 1.13E+17 | 1.13E+17 | 1.13E+17 | 1.13E+17 | 1.13E+17 | 1.13E+17 | 1.13E+17 |
| 254Cf | 1.13E+18 | 1.13E+18 | 1.13E+18 | 1.13E+18 | 1.13E+18 | 1.13E+18 | 1.13E+18 | 1.13E+18 | 1.13E+18 |

TABLE B-3. SAMPLE ORIGIN INPUT
FOR 26 KW ROD POWER

JOURN, T77, SIF, P1, B0200.
ACCOUNT, 3223, 421803032, TAK.
BEGIN, FILE, TITLE, ORIGIN, HALDEN IFA430-UPD.XJECT-26 KW \$, DUP=\$ 1\$.

REQUEST, DUM, *Q.
ATTACH(ORIGEN, ORIGEN, VIMDDJARS, ID=JGS)
ATTACH(TAPE7, CP, LIB, ADIAL, F2PAPF, ID=BG5)
RFL, EC=200.
ORIGEN(PL=10000)
EXIT(U)
REWIND(INPUT)
COPYSB.
EXIT(U)
REWIND(OUTPUT)
COPY(OUTPUT, DUM)
ROUTE, DUM, DC=FR.

HALDEN IFA-430 SINGLE PIN-MOV78-JUL79
.52686 0.204515 1.54317 1.0E-20121979 3 0 C-4

2

96

| | | | | | | | | | | | |
|--------|----------|----------|-----|----------|----------|---------|----------|-------|-----------|--|---|
| 922350 | 922350 | 942340 | | | | | | | | | |
| 541350 | | | | | | | | | | | |
| 92235 | 97.49049 | 77.87435 | 0.0 | 534.2801 | 173.7739 | .657673 | .015 | J. | 4.70E-052 | | |
| 92236 | 2.78723 | 18.4045 | 0.0 | 0.0 | .0088868 | .297004 | .015 | J. | 1.50E-042 | | |
| 94234 | 819.237 | 132.191 | 0.0 | 1452.585 | 200.304 | 1.28532 | 5.00E-03 | 0. | 5.805-052 | | |
| 54135 | 3.133E+3 | 4395.2 | 0.0 | 1.11 | .0931 | .0201 | .00851 | 0.475 | | | 2 |
| 10 | 10 | 0 | 0 | 1 | 0 | 2 | | | | | |

| | | | | | | | | | | | |
|---------------------|-----------------------|-----------------|---------|-------|-------|-------|---------|-------|------|--|---|
| 111 | 111 | 11 | 111 | | | | | | | | |
| HALDEN IFA-430 | SINGLE | PIN-MOV78-JUL79 | | | | | | | | | |
| .038 | 0.0 | .038 | .000001 | 0.0 | .038 | .012 | .000001 | 0.0 | .038 | | |
| 24. | 41.5 | 52. | 98. | 118. | 153. | 161. | 202. | 222. | 228. | | |
| HALDEN-IFA-430-JUNE | PIN-11100-97.85U-235) | 86400.DAY | | | | | | | | | |
| 1.E-3 | 1.E-3 | 1.E-3 | 1.E-3 | 1.E-3 | 1.E-3 | 1.E-3 | 1.E 6 | 1.E 4 | | | 2 |
| 922350 | .41812 | 922300 | 5.69512 | | | | | | | | |

| | | | | | | | | | | | |
|---------------------|--------------------------|-----------|------|------|------|------|------|------|------|--|--|
| 8 | 8 | 0 | 0 | 10 | 8 | 1 | 0 | 3 | | | |
| HALDEN IFA-430-JUNE | PIN STARTING | JULY79 | | | | | | | | | |
| U.U | .038 | 0.0 | .038 | 0.0 | .038 | 0.0 | .038 | 0.0 | .038 | | |
| 7. | 18. | 43. | 55. | 80. | 92. | 117. | 129. | | | | |
| HALDEN430-JUNE | PIN(11100-97.85G U-235) | 86400.DAY | | | | | | | | | |
| 9 | 9 | 0 | 0 | 9 | 0 | 3 | | | | | |
| HALDEN-IFA-430 | PIN-SHUTDOWN AND FINAL | BURN | | | | | | | | | |
| 0.0 | .026 | .026 | .026 | .026 | .026 | .026 | .026 | .026 | .026 | | |
| 60u. | 024. | 63u. | 036. | 042. | 648. | 654. | 600. | 656. | | | |
| HALDEN430 | PIN-11100 U-97.85G-U-235 | 3600. HR. | | | | | | | | | |

POOR ORIGINAL

REFERENCES

1. W. E. Vesely, et al., The RAFFLE General Purpose Monte Carlo Code, ANCR-1022, April 1973.
2. M. J. Bell, ORIGEN - The ORNL Isotope Generation and Depletion Code, ORNL-4628 (1973) (Also, with Additional Information, in CCC-217, Reactor Shielding Information Center, Oak Ridge, Tenn.)

POOR ORIGINAL

APPENDIX C

TYPICAL GAMMA RAY SPECTRUM ANALYSIS, SPECTRUM NO. 13

DATE COMPUTED 04/14/80

S.S. RELEASE TESTS FCRT-1
 0500 9 2 YOC S
 ACQUISITION TIME: 1 JAN. 3, 1980 1235131
 ENERGY CALIBRATION: OFFSET = 1.041E-01 KEV SLOPE = 4.998E-01 KEV
 QUADRATIC COEFFICIENT OF ENERGY: 0 KEV/CHANNEL
 CALIBRATION DATE: 1 JAN. 3, 1982 0 0; 0
 SAMPLE GEOMETRY: 3 CM PIPE

84533104

LINEARITY CORRECTION AT CHANNEL NUMBER PLUS 0.
 ***LINEARITY TABLE: (3) NO CORRECTION
 ***EFFICIENCY TABLE: (390) 3 CM GEOMETRY HALDEN REACTOR PGT DETECTOR

EPSLN = 0.
 EPSQD = 0.

WIDTH = 3.0000 + 0.000000(X)

RANDOM COINCIDENCE SUMMING CORRECTION = 1.00000

ENERGY AND INTENSITY CALCULATIONS

ENERGY = 1.0410000E-01 + 4.9980000E-01(X)

P, PRODUCTION MODE :
 Z, ATOMIC NUMBER :
 E, ENERGY :
 T, HALF LIFE :
 I, INTENSITY CODE :

IRRADIATION TIME = 0.000 H
 DECAY TIME = 0.000 H
 COUNTING TIME (CLOCK TIME) = .250 H
 CHANNEL ZERO TIME (LIVE TIME) = 900 S

| CHAN LOC | WID (W) | SIG (W) | AREA (COUNTS) | SIG (A) | ALL LINES COUNTING RATE (GM/SEC) | SIG (F) (KEV) | ENERGY (E) (KEV) | EFFICIENCY |
|----------|---------|---------|---------------|---------|----------------------------------|---------------|------------------|------------|
| 81.0 | | | | | | | | |
| 83.2 | 24.1 | 3.0 | 227059. | 18. | ***** | 0.00 | 41.66 | 1.5275E-04 |
| 144.8 | 3.0 | 0.0 | 8341. | 16. | 5805.469 | 0.00 | 74.97 | * |
| 162.0 | 2.4 | 0.2 | 4970. | 9. | 2944.551 | 0.00 | 81.08 | 1.8754E-03 |
| 169.5 | 3.3 | 0.4 | 7326. | 10. | 4024.334 | 0.00 | 84.82 | 2.0228E-03 |
| 212.8 | 3.0 | 0.0 | 1661. | 21. | 863.827 | 0.00 | 106.48 | 2.9606E-03 |
| 224.7 | 3.0 | 0.0 | 1353. | 23. | 589.981 | 0.00 | 112.40 | 2.6241E-03 |
| 274.3 | 3.1 | 0.2 | 130410. | 3. | 54376.688 | 0.00 | 121.66 | 2.6642E-03 |
| 277.0 | 3.0 | 0.1 | 7991. | 4. | 3341.037 | 0.00 | 136.03 | 2.6182E-03 |
| 307.8 | 3.0 | 0.3 | 34441. | 9. | 15372.185 | 0.00 | 153.95 | 2.4694E-03 |
| 311.9 | 2.9 | 0.1 | 34877. | 3. | 16393.073 | 0.00 | 165.98 | 2.3639E-03 |
| 350.2 | 3.1 | 0.1 | 68342. | 2. | 33567.800 | 0.00 | 175.15 | 2.2621E-03 |
| 394.1 | 3.0 | 0.4 | 23550. | 6. | 15719.778 | 0.00 | 197.17 | 2.0638E-03 |
| 410.6 | 2.1 | 0.6 | 6031. | 26. | 536.012 | 0.00 | 205.43 | 1.9303E-03 |
| 437.9 | 3.0 | 0.0 | 166051. | 32. | 103222.498 | 0.00 | 218.98 | 1.7939E-03 |
| 451.1 | 3.0 | 0.5 | 4805. | 20. | 2893.031 | 0.00 | 229.66 | 1.7301E-03 |
| 464.9 | 3.1 | 0.2 | 4805. | 6. | 3251.866 | 0.00 | 234.59 | 1.6488E-03 |
| 464.9 | 3.1 | 0.1 | 29370. | 3. | 20639.424 | 0.00 | 242.48 | 1.5811E-03 |
| 495.6 | 3.0 | 0.1 | 21469. | 4. | 15678.053 | 0.00 | 249.81 | 1.5215E-03 |
| 517.0 | 3.0 | 0.1 | 94700. | 4. | 72365.113 | 0.00 | 258.49 | 1.4540E-03 |
| 525.8 | 2.8 | 0.4 | 2701. | 13. | 2127.974 | 0.00 | 264.41 | 1.4104E-03 |
| 545.8 | 3.8 | 0.1 | 6278. | 4. | 5118.924 | 0.00 | 272.74 | 1.3582E-03 |
| 564.9 | 3.4 | 0.6 | 1594. | 16. | 1376.172 | 0.00 | 282.46 | 1.2930E-03 |
| 579.9 | 2.9 | 0.1 | 18588. | 2. | 16566.569 | 0.00 | 289.94 | 1.2477E-03 |

APPENDIX D

UNCERTAINTY ANALYSIS

APPENDIX D

UNCERTAINTY ANALYSIS

The uncertainty in the isotopic release rate is calculated by propagating the uncertainty of the parameters used in the equation for release rate

$$R = \frac{A f e^{\lambda t d}}{T_{\ell} \epsilon V_p B} \frac{T_D P_0}{T_0 P_D} \quad (D-1)$$

| | | | | | |
|------------|---|---------------------|-------|---|------------------------|
| where A | = | peak area | V_p | = | sample pipe volume |
| f | = | flow rate | B | = | gamma ray abundance |
| λ | = | decay constant | T_D | = | sample gas temperature |
| td | = | delay time | P_D | = | sample gas pressure |
| T_{ℓ} | = | live time | T_0 | = | 273 K |
| ϵ | = | detector efficiency | P_0 | = | 0.1013 MPa (1 atm). |

The uncertainty in R is given by

$$\Delta R = \left[\sum_{i=1}^n \left(\Delta U_i \frac{\partial R}{\partial U_i} \right)^2 \right]^{1/2}$$

where ΔU_i is the uncertainty in parameter U_i . The uncertainties, ΔU_i , used in calculating the total uncertainty in R are based on calibration results, and, for some parameters, engineering estimates based on previous experience. The fractional uncertainties (bias plus random) for each parameter are listed in Table D-1.

The uncertainty for a typical measurement is +55, -20%. The large uncertainty of P_D (Table D-1) is the dominating factor in the large uncertainty in the release rates. Instrumentation is being added to the FPMS to reduce the uncertainty in P_D to $\sim +1\%$, which will enable the uncertainty in R to be reduced to approximately $\pm 20\%$.

TABLE D-1. FRACTIONAL UNCERTAINTIES FOR RELEASE RATE CALCULATIONS

| U_i | ΔU_i | ΔU_i |
|------------|--------------|--------------|
| | (+) | (-) |
| A | 0.01 | 0.25 |
| f | 0.15 | 0.15 |
| λ | 0.01 | 0.01 |
| t_d | 0.20 | 0.20 |
| T_d | 0.10 | 0.10 |
| ϵ | 0.15 | 0.15 |
| V_p | 0.20 | 0.20 |
| B | 0.10 | 0.10 |
| T_D | 0.03 | 0.02 |
| P_D | 1.00 | 0.01 |